CONTROLS ON NAPL MIGRATION PATHWAYS IN A MIXED-WASTE RAIL YARD, DUNSMUIR, CALIFORNIA

By

LAUREN N. GUIDRY

Bachelor of Science in Geology

Oklahoma State University

Stillwater, OK

2012

Submitted to the Faculty of the
Graduate College of the
Oklahoma State University
in partial fulfillment of
the requirements for
the Degree of
MASTER OF SCIENCE
December, 2015

CONTROLS ON NAPL MIGRATION PATHWAYS IN A MIXED-WASTE RAIL YARD, DUNSMUIR, CALIFORNIA

Thesis Approved:

Dr. Todd Halihan

Thesis Adviser

Dr. Estella Atekwana

Dr. Garey Fox

Dr. Javier Vilcaez Perez

ACKNOWLEDGEMENTS

First, I would like to give infinite thanks to my advising professor, Dr. Todd Halihan, for his continuous patience and endless knowledge of hydrogeology. Additionally, I would like to thank the rest of my thesis committee, Dr. Estella Atekwana, Dr. Garey Fox, and Dr. Javier Vilcaez Perez for their insightful comments and educational support.

I would like to thank CH2M and Aestus, LLC for providing the opportunity to assist in this environmental investigation and also for performing field operations and data collection. Additional thanks goes to Boone Pickens School of Geology at Oklahoma State University for providing the resources to complete this project.

Additionally, I would like to thank my friends and family for their continued support throughout the entirety of this research.

Name: LAUREN N. GUIDRY

Date of Degree: December, 2015

Title of Study: CONTROLS ON NAPL MIGRATION PATHWAYS IN A MIXED-WASTE RAIL YARD, DUNSMUIR, CALIFORNIA

Major Field: GEOLOGY

Abstract: On a rail yard site impacted with multiple spills of nonaqueous phase liquids (NAPLs), NAPL was actively being transported in a subsurface pathway to a nearby stream. While significant quantities of NAPL were immobile on the site, further understanding of the active pathway requires understanding the site transport mechanism(s). The mixing of surface water and groundwater, and the flow conditions capable of producing a suitable environment for biochemical processes were evaluated. Additionally, a hydrogeophysical framework for evaluating sites with multiple long-term impacts was suggested. Evaluation of the site was performed by data integration of geophysical, geochemical, and hydrogeologic data. Geophysical data included 71 electrical resistivity imaging (ERI) datasets across the site. Geochemical data included onsite well data, stream data, and regional well data. Hydrogeologic data included borings and head data incorporated into a site groundwater model. These datasets were used to generate a GIS database of site data to produce maps of site parameters relative to geophysical and geologic features. Additionally principal component analysis (PCA) and end-member mixing analysis (EMMA) were used to identify anomalous wells for the site.

Results of the hydrogeologic analysis indicates during high stream flow events, groundwater chemical constituents become homogenized and diluted across the site. During baseflow, chemical constituents increase in concentration in the northern end of the site due to biodegradation. The results of the EMMA analysis demonstrate geochemical constituents in the northern area of the field site were outliers from the regional and onsite samples. The southern end of the site, while impacted, reflects concentrations of background waters. This complex surface water/groundwater mixing process at the site periodically dilutes the thermally active environment, which appears to be required to mobilize NAPL. A revised hydrogeophysical framework for characterizing future sites is discussed.

TABLE OF CONTENTS

LIST OF TABLES

Table Page

LIST OF FIGURES

Figure Page

CHAPTER I

INRODUCTION

The migration of immiscible hydrocarbon in a groundwater setting can be caused from many mechanisms, including abiotic and biotic processes (Bedient et al., 1999; Lee et al., 2001). However, efforts to understand nonaqueous phase liquid migration to surface water are less common. Additionally, many modern impacted sites are mixtures of multiple sources that are from different eras. In these complex geologic settings with aged mixed hydrocarbons and surface water interactions, determining migration mechanisms can be problematic.

Research on transport pathways based on hydrogeologic controls has been extensively investigated (Newell et al., 1995; Fetter, 1999; Miller et al., 2014). Geologic mechanisms can create a preferential migration pathway(s) for contaminants due to lithology and/or stratigraphy (Bedient, 1999; Fetter, 1999). However, without considerable heterogeneity in the subsurface geology, understanding the controls on a migration pathway become more focused on hydrogeologic and biogeochemical factors (Poole et al., 2006; Spence et al., 2005; Newman et al., 1998). Previous investigations have demonstrated flow pathways defined by a mixing of surface water and groundwater, such as a hyporheic zone or a biochemical mixing zone (Wondzell and Swanson, 1996; Malard et al., 1999; Wroblicky et al., 1998). Flow pathway(s) can become active during baseflow conditions, while during high stage conditions can form broad-scale flows that flood the gravel media in coarse alluvial settings (Miller et al., 2014). Additionally, dispersion

through the site can influence the flow. As background waters input into the site the amount of each water coupled with their magnitude and direction can create a dominant pathway (Doctor et al., 2006; Valder et al., 2012).

The study area of this research is a century old rail yard in Northern California with hydrocarbon impacts across the site (Figure 1). Sheens appear on an adjacent stream periodically due to NAPL transport from undefined mechanisms through a preferential pathway through the site. The appearance of NAPL in extraction wells and the appearance of oil sheens in the adjacent stream are indicators that the site has an active NAPL migration process. The migration of nonaqueous phase liquids (NAPLs) in the subsurface is affected by abiotic and/or biotic processes, such as groundwater flow or biodegradation (Lee et al., 2001). Previous characterization of the NAPL extent at the research site provides a dataset to identify the primary mechanisms of NAPL migration in a preferential flow pathway. Previous site reports describe the site as having widely distributed NAPL throughout the site with observations of NAPL contamination in 24 of 27 borings and 7 of 12 wells. Additionally, electrical resistivity imaging (ERI) data shows an anomalously low linear bulk resistivity (high bulk conductivity) zone through the site. Understanding the research site with significant quantities of immobile contamination helps to develop hypotheses on localized NAPL migration pathways. The isolated output of the oil sheens to the stream coupled with well, soil core, and geophysical data, support that NAPL migrates through a pathway caused by mechanisms that are both abiotic in nature (the mixing process), as well as biotic (the degradation of hydrocarbons).

The field site for this study is contaminated with diesel-range organics and oil-range organics that are transporting into the adjacent river. Previous reports suggest the NAPLs are migrating beneath a concrete retaining wall adjacent to the stream (Figure 1). This is evidence the contaminant plume is diving well below the water table. Factors capable of creating a diving plume can influence contaminant transport (Weaver and Wilson, 2000; Nichols and Roth, 2006).

Additionally, byproducts of biodegradation provide insight into the site biochemical reactions taking place and provide a better understanding of drivers of NAPL transport (Bennett et al., 1993; Lee et al., 2001; Fan et al., 2011).

Utilizing several methods, the aim of this research is to gain a better understanding of the hydrogeologic mixing of surface water and groundwater, and the ongoing biochemical processes at the site to distinguish the mechanisms of a NAPL migration, as well as providing a framework for investigation on other similar sites near water bodies. Complex system frameworks to evaluate these sites with a number of possible transport mechanisms are limited, and testing a hydrogeophysical framework for evaluation is an important step in addressing these types of sites. A hydrogeophysical framework would be a suitable means for evaluating sites with multiple long-term impacts.

HYPOTHESIS

For this site a number of potential transport mechanisms exists to migrate NAPL from groundwater to the surface water. The hypothesis for the site is that the NAPL pathway can be explained from the mixing of surface and groundwater shown through the physical and geochemical gradients across the site. As these waters interact, they produce an environment suitable for microorganisms to biodegrade and mobilize previously immobile NAPL through either biotransformation and/or biosurfactant production. The river water is enriched in electron acceptors (e.g. oxygen, nitrates, manganese, iron, sulfates) and contributes to the replenishing of chemical constituents needed for microbial respiration. Additionally the stream water, including high stream discharge events, is hypothesized to produce hydrogeologic conditions, such as high stage flow, affecting the transport of NAPL. These differences in waters would produce distinctive gradients on the site and indicate the spatial area of electron acceptor input. This

information would provide further evidence that the site has multiple hydrologic inputs and conditions favorable for periodic NAPL transport to surface water.

OBJECTIVES

The objectives of the proposed research are to (1) determine if and where groundwater and stream water influence the distribution and concentration of physical and chemical parameters and contaminants at the site, (2) determine if and where biochemical processes are influencing the site, and (3) evaluate the hydrogeophysical framework employed for evaluating similar sites.

The project objectives will be achieved by conducting a literature review, data analysis, and statistical analysis to (1) determine the techniques used to measure for transport mechanism of NAPL and apply to the field site with the available data, (2) document the changes in major physical and chemical parameters, such as temperature, pH, and major ions, across the field site compared against regional water quality in both surface and groundwater, (3) evaluate the mixing of each source water from the composition of site water, including major ions and metals, and (4) isolate the areas of potential biochemical processes operating on the site.

RESEARCH SIGNIFICANCE

This section includes the value of the conducted research and the reason for it is significance, both on intellectual merit and broader impact. The anticipated results will provide a framework for characterizing mixed waste sites with preferred pathways for migration of NAPLs. This research will contribute to the understanding of the physical, chemical, and possibly

biological mechanisms that influence NAPL migration pathways on a site with unique properties for evaluating these mechanisms in a data integration hydrogeophysical framework.

The broader impact of this research is to provide an understanding of the approach to site characterization for a large class of mixed waste sites with NAPL migration pathways. Additionally, NAPLs are known to continually degrade groundwater and surface water quality posing a potential threat to biotic systems (Sudsaeng et al., 2011). This research will aid in understanding how to manage the environmental impact fueling and storage locations produce throughout a lifetime of use.

CHAPTER II

LITERATURE REVIEW

NAPLs are generally categorized by their specific gravity as light non-aqueous phase and dense non-aqueous phase liquids (LNAPLs/DNAPLs), which can be present in the vadose and saturated zones (Newell et al., 1995). LNAPLs often stay in the unsaturated zone or spread laterally on top the water table and migrate in the direction of groundwater flow (Hunt et al., 1988; Lee et al., 2001; Sudsaeng et al., 2011). DNAPLs move through the vadose and saturated zones until a confining unit is reached then move along the slope surface (Hunt et al., 1988; Fetter, 1999).

MECHANISMS OF BASIC NAPL TRANSPORT

The basic theory of Darcian groundwater flow is discussed by multiple practitioners in the field (Bedient, 1999; Fetter, 1999; Fitts, 2002). However, to better understand the theory of multiphase flow a brief overview of the basic transport mechanisms generally applicable to field cases will be presented. Groundwater flow can be described using Darcy's law for laminar flow; however, the equation has to be modified to account for multiple phases, aqueous, nonaqueous, and gas, in a steady-state saturated flow environment (Fetter, 1999) from

$$Q = \frac{-k_r k_i \rho}{\mu} A \frac{dh}{dl} \quad (1)$$

where Q is the volume of the fluid (L^3/T), k_r is the relative permeability of the fluid, k_i is the intrinsic permeability of the media (L^2), μ is the dynamic viscosity of the fluid (MT/L^3), A is the cross-sectional flow area (L^2), dh/dl is the gradient of the head of the fluid (L/L), and ρ is the density of the fluid (M/L^3). This equation accounts for the multiple phases within a system. It is influenced by flow velocity, density, viscosity, permeability, and the volume of NAPL present.

The controlling factors governing the migration of NAPLs can be grouped into pore-scale and field-scale migration mechanisms. Pore-scale migration controls include density, viscosity, interfacial tension, wettability, capillary pressure, saturation, and relative permeability (Newell et al., 1995; Bedient, 1999). These parameters can greatly influence the mobility of NAPL and can be affected by factors such as temperature, pH, surfactant concentration, NAPL composition, mineralogy, and/or dissolved gases, which could increase or decrease the NAPL mobility (Newell et al., 1995).

Field-scale migration controls include properties of NAPL, release rate, contaminated area, lithology and stratigraphy, and properties of the aquifer (Newell et al., 1995; Bedient, 1999). NAPL volumes released in sufficient quantities in unsaturated soil will percolate downward through the vadose zone and become mobile through the porous or fractured media with the groundwater flow direction (Abdul, 1988; Hunt et al., 1988; Jackson et al., 2006). However, if there is limited NAPLs, the migration will be inhibited by forces such as interfacial tension and leave behind residual NAPLs (Fetter, 1999). The subsurface geology can provide pathways of least resistance to enable the migration of NAPLs. Different types of lithology provide variability in grain sizes and grain sorting causing aquifer heterogeneity. The variability in the lithology will influence the fluid velocity and dispersion rates, defined as hydrodynamic dispersion (Fetter,

1999). This influences the direction and magnitude of fluid through the porous media producing pathways for NAPL migration. The stratigraphy can also be influential in migration, i.e. if there are impermeable zones, the direction of dipping beds, the fracture network (Abdul, 1988; Newell et al., 1995; Bedient, 1999; Fetter, 1999).

MECHANISMS OF DIVING PLUMES

A diving plume is defined as the downward vertical migration of a contaminant plume in the subsurface with increasing depth from the initial source (Weaver and Wilson, 2000; Nichols and Roth, 2006). They are commonly dismissed for LNAPLs as the assumption is made that they will not migrate below the water table, although the assumption is incorrect. Diving plumes are controlled by both hydrogeological and non-hydrogeological factors (Griesemer, 2001; Nichols and Roth, 2006). The factors that induce a downward vertical gradient include (1) a higher elevation of the water table with respect to the local discharge areas, (2) an increase in hydraulic conductivity with depth, (3) a high infiltration rate for precipitation and/or runoff, and (4) a significant time period, allowing dispersive forces to transport NAPL (Weaver and Wilson, 2000; Griesemer, 2001; Nichols and Roth, 2006). Griesemer (2001) notes that during high precipitation events upward vertical migration to discharge areas may occur after a plume had migrated below the water table.

Additionally, diving plumes are affected by the rate of vertical dispersion. High vertical dispersion rates would cause LNAPL to expand relatively close to or at the water table. If a site remains unmitigated the plume would be present over a longer period of time allowing effects of recharge, hydraulic gradient, and dispersion to displace the plume to a greater extent (Griesemer, 2001). It is important to note geological and biological factors will affect the diving plume by

means of dipping beds, preferential flow paths, anisotropy, and concentration gradients caused from biodegradation (Nichols and Roth, 2006).

MECHANISMS OF BIODEGRADATION

Biological mechanisms influencing NAPL migration are grouped into two categories: biodegradation and biosurfactants. The U.S. Environmental Protection Agency (United States Environmental, 2012a) defines biodegradation as the process of transformation or alteration of the chemical structure of a substance into different compounds through actions of microorganisms. Biodegradation of NAPLs can occur aerobically or anaerobically, depending on the aquifer conditions (Rifai et al., 1988). The type of degradation depends on a series of biochemical reactions governed by the limit of essential nutrients and/or the availability of electron donors and/or acceptors, such as oxygen (Rifai et al., 1988; Fan et al., 2011). These nutrients and electrons provide microbial populations energy to synthesize biomass and maintain life. The order of electron acceptors to be utilized in the subsurface is commonly $O_2 > NO_3 > Mn^4 > Fe^3 > SO_4$ (Fan et al., 2011). Oxygen is the preferential electron receptor during biodegradation and can be sourced from the mixing of horizontal and vertical flows, as oxygen will move into the center of the plume. The rate of biodegradation will increase with increasing oxygen availability, which is dominated by groundwater velocity. However, the rate of microbial consumption of oxygen is often much faster than the rate of oxygen delivery. This rate difference can cause the development of anaerobic conditions, limiting specific types of biodegradation (Rifai et al., 1988). The types of biodegradation influence the biotransformation of NAPL and the rate of transport through a porous media (Rifai et al., 1988).

Additionally, biodegradation rates depend on the viscosities and densities of the NAPLs present. Lower densities and viscosities create conditions for an increase in biodegradation rates

as they are associated with smaller molecules (Birman and Alexander, 1996). Temperature can also strongly influence the rate of biodegradation. Birman and Alexander (1996) discuss the increase in temperature from 22°C to 28°C greatly increased the extent of biodegradation of NAPLs. Additionally, Leahy and Colwell (1990) discuss the increase in biodegradation associated with an increase in temperature; however, they state the drastic difference lies between temperatures of 30°C to 40°C.

Commonly defined as surfactants, natural surface-active agents (e.g. detergents) are produced by microorganisms (Banat, 1995; Ron and Rosenberg, 2001). Many of these agents reduce surface tension and interfacial tension of aqueous and nonaqueous mixtures. Due to the lowering of tension, emulsification can occur causing the continuous NAPL to break up and migrate with the flow of the surrounding aqueous solution (Banat, 1995; Atekwana et al., 2004b). Biosurfactants are generally associated with hydrocarbon uptake, from hydrocarbon-degrading microorganisms, as seen from their spontaneous releases and their primary functions (Banat, 1995). Biosurfactants are influenced by several factors including, the nature of the carbon substrate, the concentration of essential nutrients, and the culture conditions. The essential nutrients can be defined as nitrogen, phosphorous, magnesium, iron, and manganese ions. The culture conditions for the microorganisms can be influenced by pH, temperature, agitation, and dilution rates (Banat, 1995).

GEOPHYSICAL EVALUATION OF NAPLS

NAPLs are usually more electrically resistive than surrounding fresh groundwater. This is due to the partial replacement of pore waters with NAPLs decreasing the conductivity (Atekwana et al., 2004b), and the blocking of current flow (Sefa, 2015). However, the presence of microbial activity could increase the conductivity (Atekwana et al., 2004b). As biodegradation occurs the

microbes produce organic acids (Cassidy et al., 2001). The organic acids then interact with the surrounding rocks and enhance chemical weathering. The dissolution of minerals causes an increase in dissolved solids, increasing the conductivity. Total dissolved solid (TDS) values primarily are derived from elevated concentrations in calcium, sodium, magnesium, silica, and bicarbonate ions (Legall, 2002). It is important to note that higher TDS values can also result from geologic heterogeneity and an increase in water saturation (Atekwana et al., 2004a).

Additionally, elevated conductivity could be caused from the growth and metabolic activities of microbial populations. Microorganisms colonize on sediment grains altering the chemical and physical surroundings by producing biofilms and nanowires. Specific microorganisms have highly conductive nanowires, which may influence the subsurface conductivity levels (Allen et al., 2007). The transport of contaminants can be affected by the type of minerals and microorganism present in the subsurface. The transport of NAPL can be significantly enhanced with the presences of mobile microorganisms rather than microorganisms adsorbed onto minerals in the subsurface (Abdel et al., 2009).

CHAPTER III

SITE DESCRIPTION

The site is a historic locomotive diesel and bunker C fueling and maintenance station in operation since the late 1800s, approximately 640 m (2,100 ft) in length, and 120 m (390 ft) in Dunsmuir, California (Figure 1and 2). Many remediation techniques have been used to treat NAPLs in the groundwater at this site (Bedient et al., 1999). In the 1920s, upon the discovery of the groundwater impact, there were efforts to reduce the flow of the NAPLs to the stream by constructing a concrete retaining wall (Figure 3). However, the wall was not anchored into bedrock and the groundwater flow paths migrated around and below the wall to continue transporting contaminants into the river. In 1971 the first groundwater extraction and treatment system was installed. This included eight extraction wells, an infiltration gallery, a surge pond, and treatment system. This operated until 1992 and a year later a new groundwater extraction system was implemented and continues to date. The latest system added an additional 18 extraction wells, an 850 ft long interceptor barrier trench to the base of the retaining wall, a polyethylene liner for the wall, and a new treatment system. This groundwater system includes a barrier system but does not reach the depth of bedrock and has resulted in an increase in the water table elevation behind the barrier (Figures 3 and 4). NAPLs continue to be transported to the stream approximately 100 years later. Significant quantities are still present across the site and seeps into the stream over a 140 m (450 ft) segment of stream bank (Figure 5). Sheens are periodic and discontinuously visible in the stream. On the walk way of the retaining wall NAPL

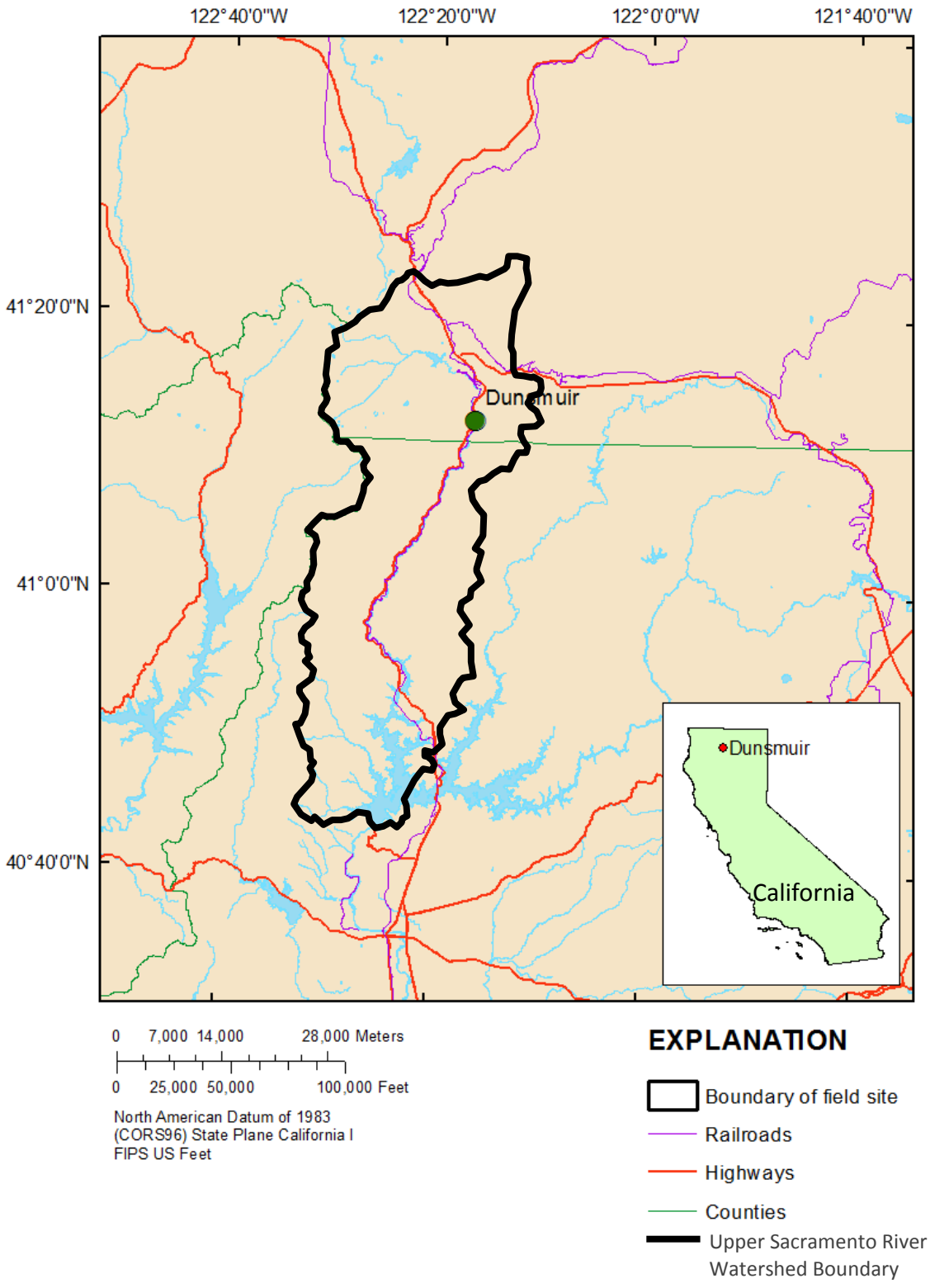

Figure 1. Site location of rail yard, city of Dunsmuir, and Upper Sacramento River watershed, inset map shows location in California (modified after Garber, 2009).

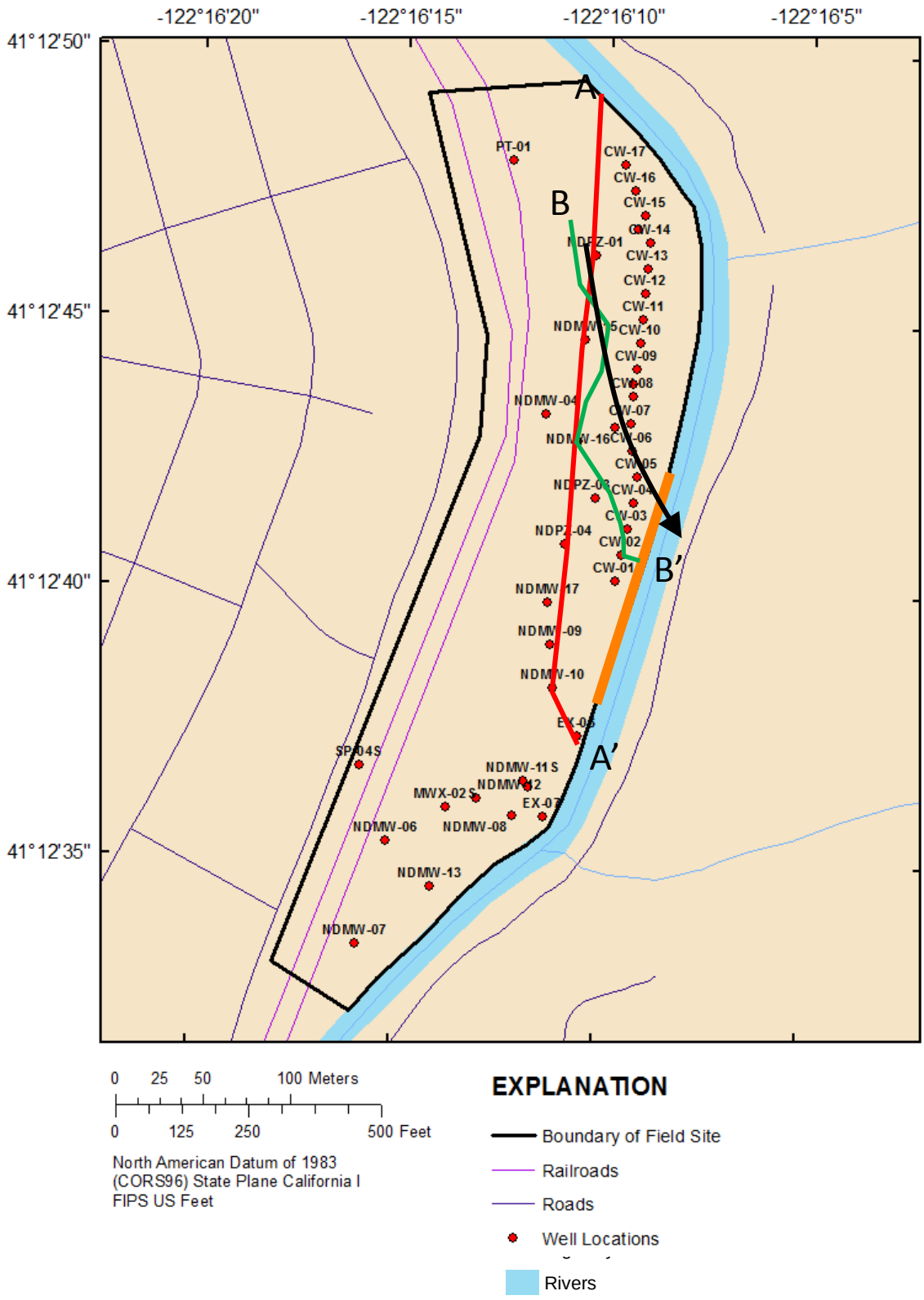

Figure 2. Site schematic showing well locations in relation to the river and railroads, orange line indicates the 450' segment with NAPL seeps, black arrow shows NAPL flow pathway, red line is for cross section in Figure 6, green line is for cross section in Figure 10.

Figure 3. Image of the latest retaining wall during the installation of the groundwater extraction and treatment system from the 1990s (Gentry et al., 2013).

Figure 4. Image of groundwater extraction and treatment system during installation during the 1990s (Gentry et al., 2013).

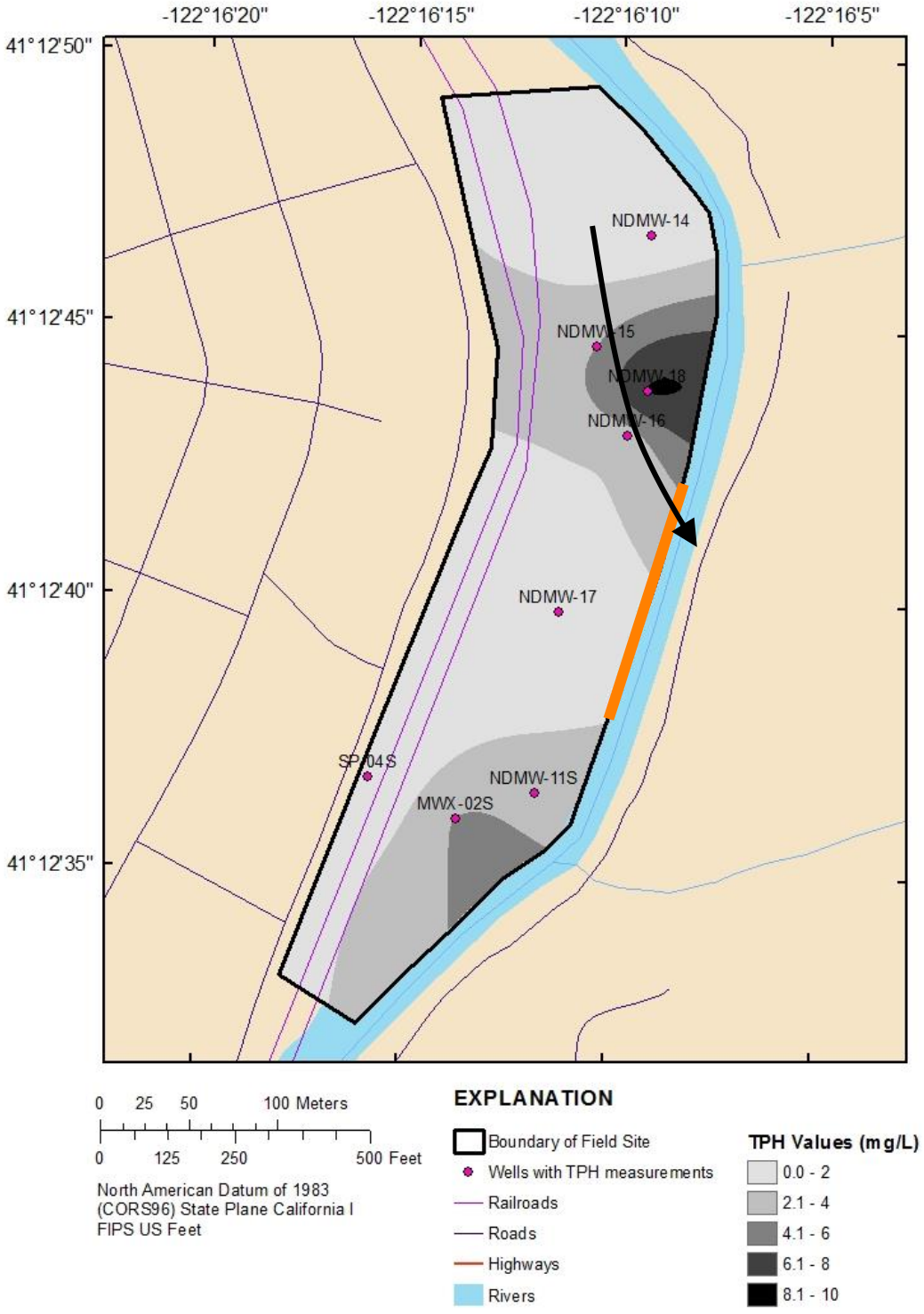

Figure 5. Map showing the distribution of Total Petroleum Hydrocarbon (TPH) quantities across the site. Black arrow indicates the transport pathway, orange line indicates the 450' segment with NAPL seeps.

seeps were observed on the concrete as well as the grout tubes located along the walk way adjacent to the stream.

GEOLOGY

Regionally, the study site is within the Cascade chain in the Pacific Northwest (Baker et al., 1994). The site is adjacent to the Sacramento River in a steep valley located in northern California near the southwest edge of Mount Shasta (41°24'36.84" N, 122°11'42.98" W; Figure 1). Mount Shasta is a stratovolcano of diverse composition, primarily basaltic and andesitic with minor dacite flows (Williams, 1932; McBirney and White; 1982; Driedger and Kennard, 1986; Streck et al., 2007). At present, Mount Shasta shows low-levels of geothermal and seismic activity (Hirt, 1999). Locally, the study area is within a narrow river-dominated valley with steeply dipping topography on both sides of the rail yard. The steep topographic gradients around Dunsmuir strongly influence the flow of water into the site (Cirmo and McDonnell, 1997). The site is composed of man-made fill, consisting of washed river rock, overlying Quaternary alluvium, consisting of unconsolidated course-grained igneous gravel and sand, approximately 4 to 8 m thick (15 to 25 ft; Figure 6). The bedrock is composed of gabbro and diorite from the Ordovician as part of the Eastern Klamath Belt and is approximately 6 to 9 m (20 to 30 ft) below the surface (Wagner and Saucedo, 1987). The elevation of the water table is approximately 2 to 4 m below the surface.

HYDROGEOLOGY

The southwest side of Mount Shasta is in the Sacramento River drainage area (Figure 1). The drainage area is supplied by snowmelt and glacial meltwater. Runoff from the volcano supplies intermittent streams within the drainage area, eventually contributing to the Sacramento

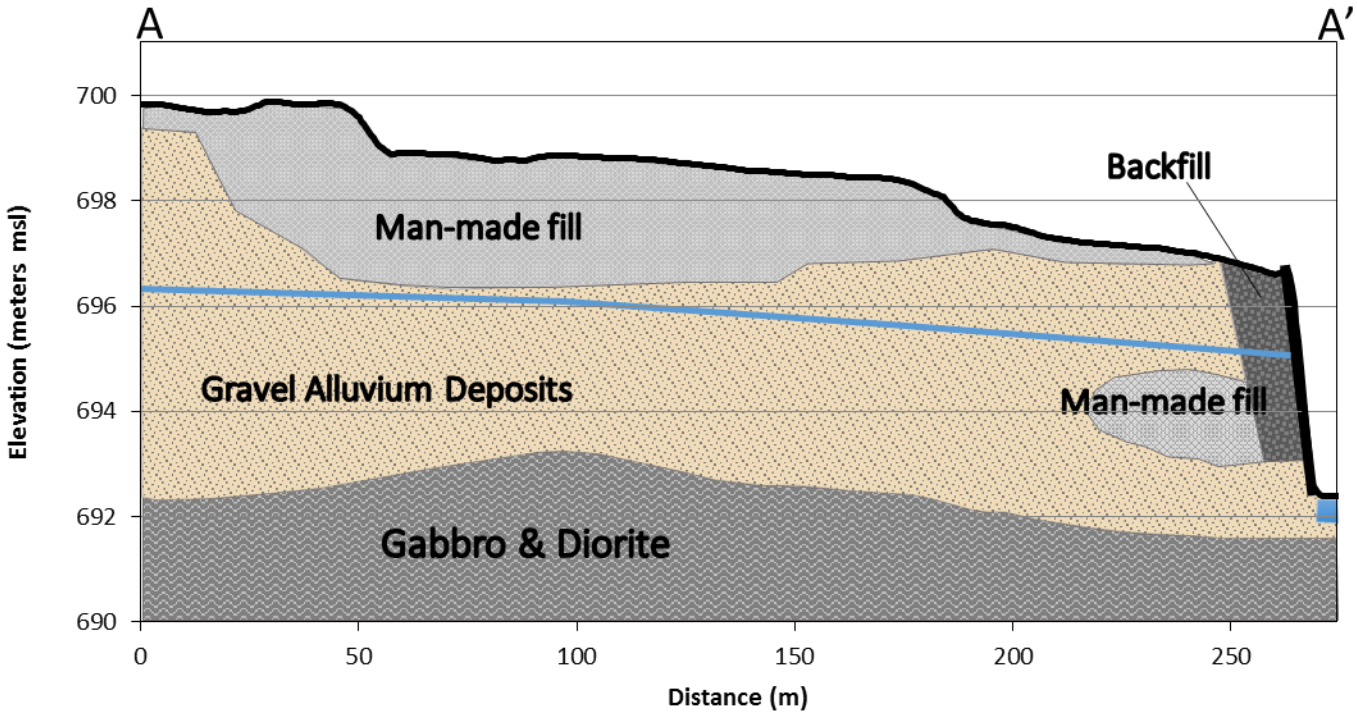

Figure 6. Cross-section showing the lithology and water table (blue line) from A to A' trending northwest to southeast to the Sacramento River (modified from Garber, 2009). See Figure 2 for location of cross section.

River. The Sacramento River flows south and is directly adjacent to the field site on the east side. Additionally, the porous volcanic rocks within the drainage area allows for groundwater flow and discharge to the river (Driedger and Kennard, 1986). River input and precipitation contribute to seasonal fluctuations in groundwater levels. Previous site reports indicate levels fluctuate up to 2.5 m (8 ft) seasonally and groundwater velocities range from $1.3x10^{-4}$ to $2.8x10^{-4}$ m/s (38 to 80 ft/day). A groundwater model developed for the site indicates significant elevation differences between the northern and southern end of the field site and groundwater flow from northwest to southeast (Gentry et al., 2013).

GEOPHYSICS

Previous site reports indicate electrical resistivity imaging (ERI) was completed using Aestus' GeoTrax Surveys. A total of 71 surveys were performed at the field site. ERI surveys show a range of electrical resistivity measurements (Figure 7). The two-dimensional survey images were utilized to determine the areas of decreased resistivity, indicating potential pathways of NAPL migration on the site (Figure 8 and 9). Areas of decreased resistivity tend to indicate the weathering of NAPLs from microbial activity (Halihan et al., 2005). The conductive areas form a sinuous pathway through the field site to the stream, where the sheen is present. The geophysical data were used in this research to determine the NAPL migration pathway. This was conducted by isolating continuous zones of high conductivity (arrow in Figure 7).

Previous reports indicated completion of 6 newly drilled wells along the path for a total of 12 wells along the conductive pathway. Additionally, the 12 wells located within the ERI conductive pathway were all found to have NAPL. The NAPL increased in depth with proximity to the concrete retaining wall and in some wells was over 2 m (7ft) below the water table (Figure 10). The significant amount of NAPL below the water table provides evidence of the movement

of the NAPL plume downward. Previous chemical fingerprinting indicated the NAPLs in the stream were most similar to NAPLs located within the conductive pathway.

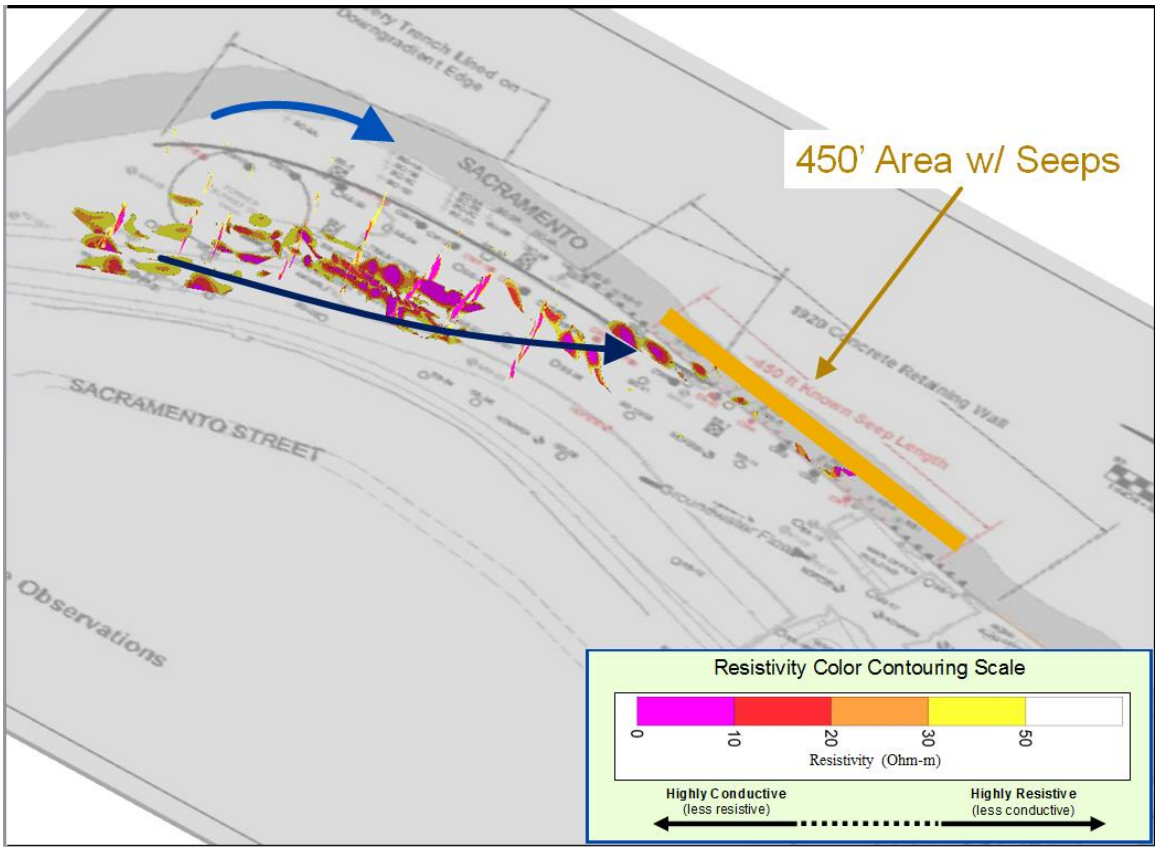

Figure 7. Fence diagram showing 2D ERI transects with low resistivity (<50 Ohm-m) data along confirmed LNAPL flow path. The dark blue arrow shows the location of the dominant pathway through the field site identified by the continuously high ERI conductivity measurements (site model from Aestus, LLC, 2011).

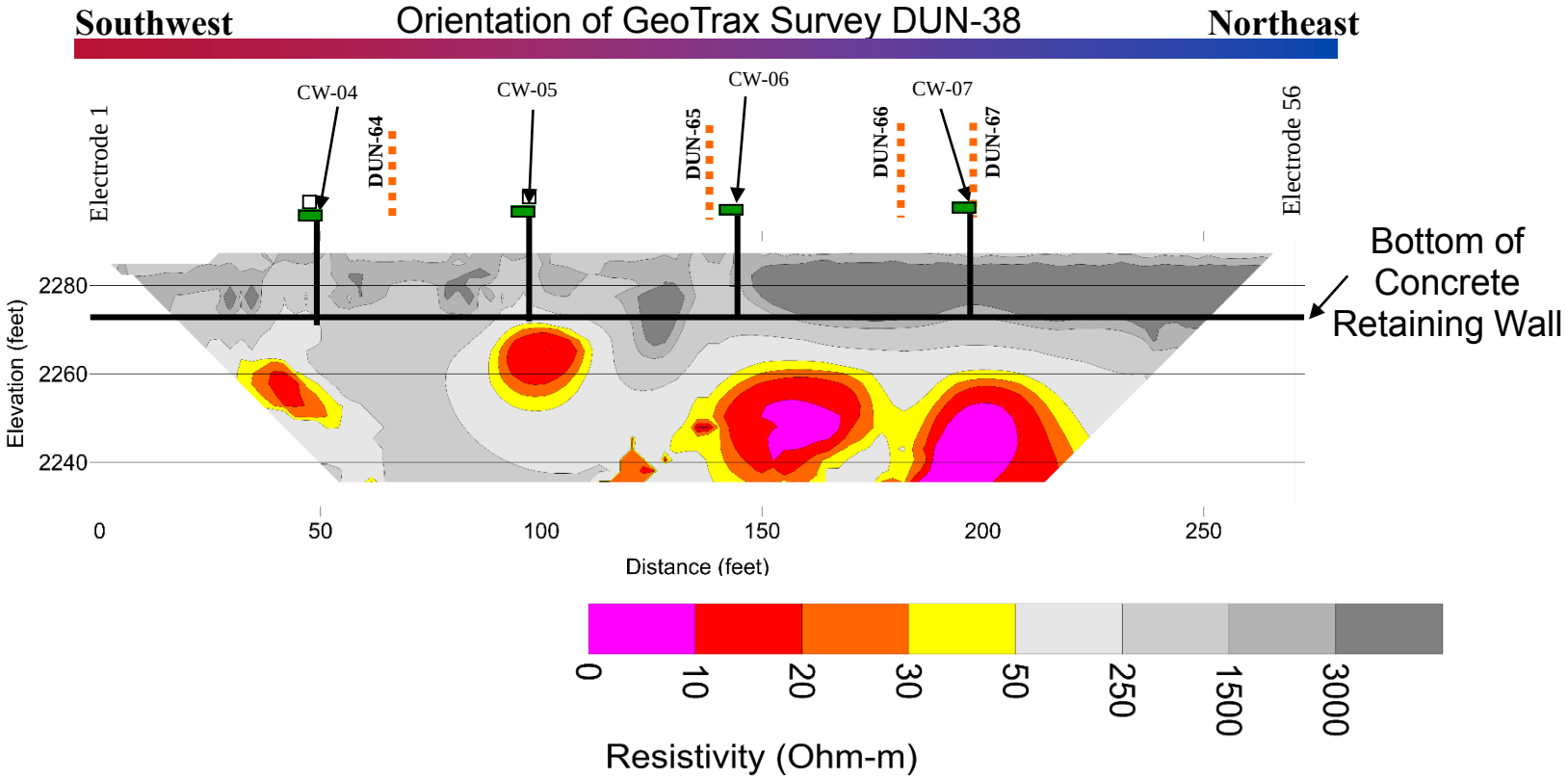

Figure 8. ERI 2D transect at the site adjacent to the river showing the conductive pathway below the concrete retaining wall measured October 21, 2010 during a period of baseflow. The adjacent river was at 225 cfs (Aestus, LLC, 2013). Orange dashed lines indicate perpendicular ERI transects, black vertical lines indicate collection wells designated CW.

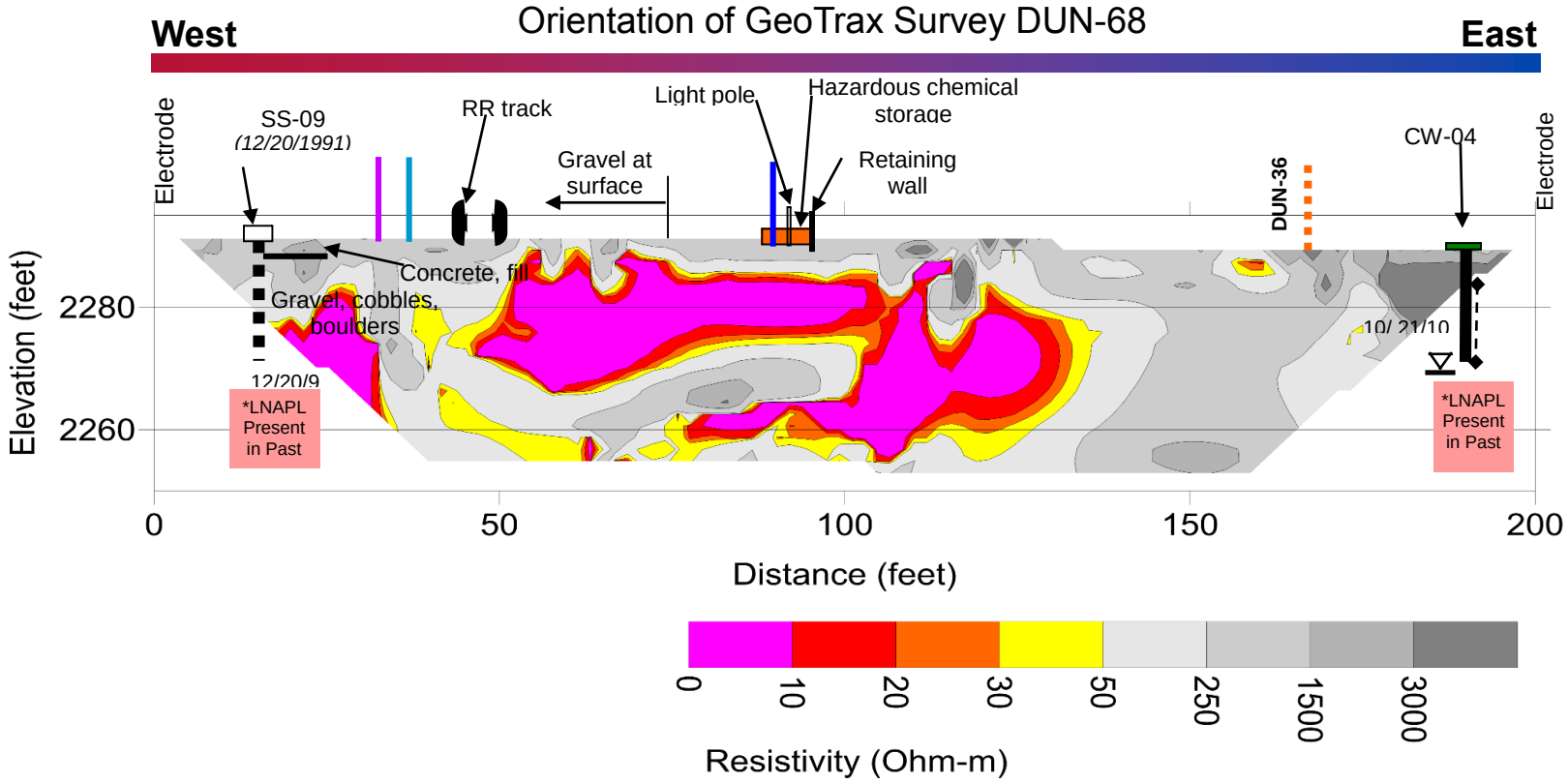

Figure 9. ERI 2D transect at the site adjacent to the river showing the conductive pathway below the concrete retaining wall measured October 21, 2010 during a period of baseflow. The adjacent river was at 225 cfs (Aestus, LLC, 2013). Orange dashed lines indicate perpendicular ERI transects.

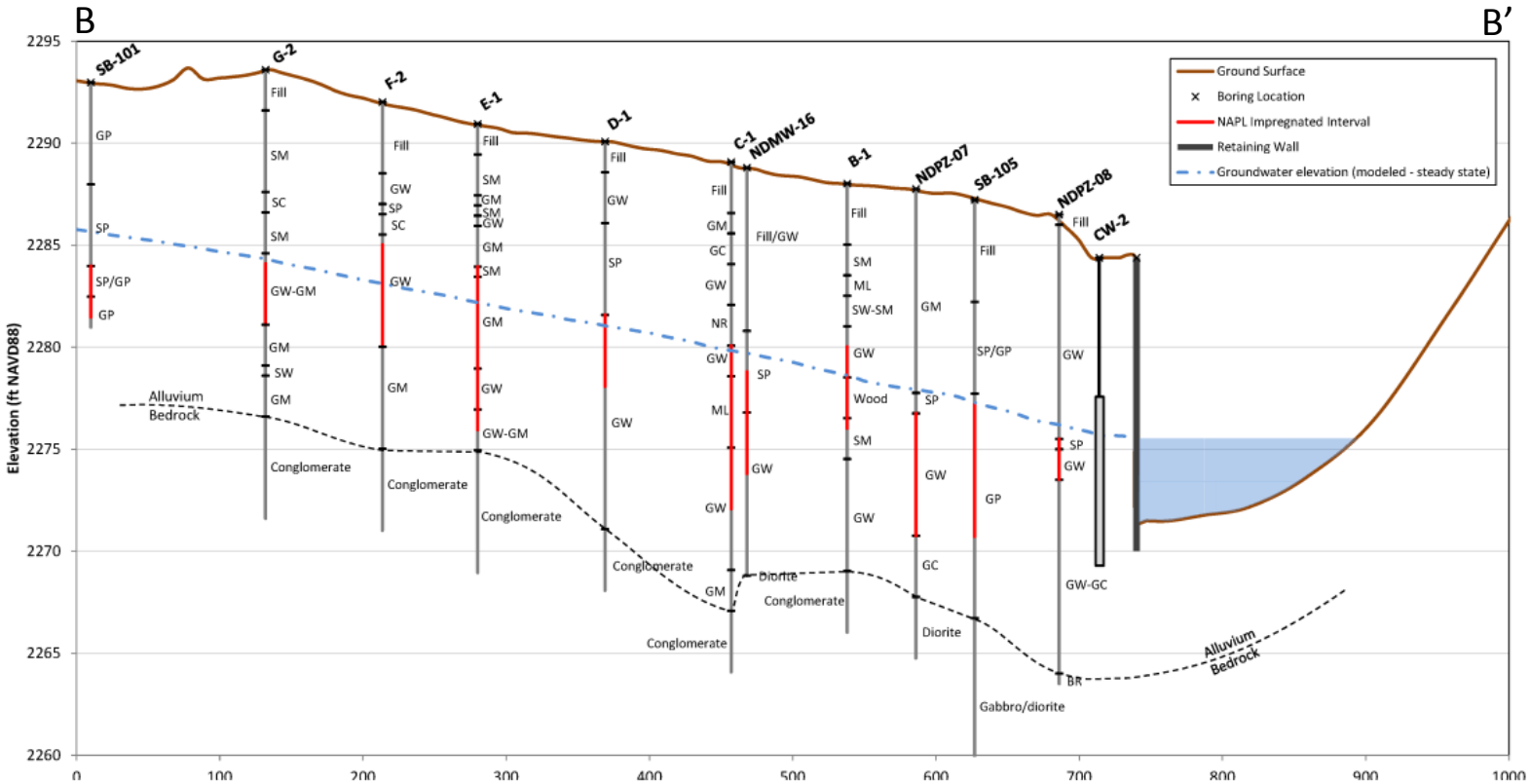

Figure 10. Cross-section showing the location of wells within the conductive pathway visible on ERI (Gentry et al., 2014). Abbreviations are; BR (bedrock), GC (clayey gravels), GM (silty gravels), GP (poorly graded gravels, GW (well-graded gravels), ML (inorganic silts and very fine sands), NR (not recognizable), SC (clayey sands), SM (silty sands), SP (poorly graded sands), SW (well-graded sands).

CHAPTER V

METHODS

Primary factors influencing migration were determined using multiple analyses, including basic hydrogeology and NAPL transport and statistical mixing analysis. It is important to note that all site data acquisition was preformed prior to this research; however, regional water data was acquired from the USGS database and the State of California (United States Geological, 2014).

BASIC HYDROGEOLOGY

A significant amount of data was used from the site, including basic groundwater parameters, such as depth to water, temperature, and fluid electrical conductivity. Previously collected chemical properties are available, including major anions, Benzene-Toluene-Ethylbenzene-Xylene (BTEX) concentrations, and chemical finger-printing of extractable petroleum hydrocarbons (EPH) and volatile petroleum hydrocarbons (VPH). These datasets were analyzed and correlated to identify trends and anomalies, which were used to develop evidence for the most influential mechanisms contributing to NAPL transport, using ESRI ArcMap, binary plots, principal components analysis, and end-member mixing analysis.

Geology

To determine the geologic influence on NAPL migration, the geology of the subsurface was examined using soil and well logs, geological surveys, and previously described sections of the site (Lee et al., 2001). The lithological descriptions at specific depths were used to create a conceptual cross-section of the site (Figure 6). Understanding the geology and stratigraphy provides insight on the site characteristics, including if a preferential flow path(s) exists due to the existence of coarse-grained channels.

Physical Hydrogeology

Some initial site characterization was performed to develop a basic understanding of the site. This was accomplished by creating an ESRI ArcGIS database to analyze the datasets. Background regional layers were downloaded from the USGS, including hydrology overlays, roads, railroads, and government boundaries. Previously measured datasets were then imported into ESRI ArcGIS. The datasets were interpolated into a continuous surface (raster) by using Topo to Raster within the 3D analyst Toolbox (ESRI, 2001). The spatial extent of the raster was limited to a polygon designating the site boundary. The datasets processed using this method were water elevations, temperature, and chloride (Cl) for basic site hydrogeology.

Previous measurements of groundwater elevation were taken from 2009 to 2010 with five sample dates for eleven wells. Similarly, previous temperature measurements were taken from 2009-2010 with eleven sample dates for eleven wells. Temperature was also previously recorded from transducer data, including stream data and three wells on six hour intervals for eight months. The temperatures from the river were compared to the site wells. The data were evaluated for spatial and temporal trends to determine seasonal effects and/or site variability.

There is a single sample date for pH measurements on July 21, 2011 from eight wells. These mapping methods are based from the concentration contour map created by Bennett et al.

(1993), which show the areas with elevated concentrations. Additionally, examination of the concentrations over time was analyzed by Bennett et al. (1993), which show seasonal variations. Groundwater and surface water data were downloaded from the USGS National Water Information System (United States Geological, 2014). These data were used to map the spatial distribution of regional groundwater and stream water temperatures and pH in comparison to site data. A table was created to examine the differences between the regional and the site data.

Groundwater Mixing

Understanding where the waters at the field site are sourced determines the amount of mixing taking place and the most influential source. To determine the source(s) of the mixed water at the field site a principle components analysis (PCA) was performed using Minitab (Christophersen and Hooper, 1992; Doctor et al., 2006). This multivariate approach allows the comparison of multiple parameters at once, providing the variables with the most variance, the principle components (Doctor et al., 2006; Cloutier et al., 2008). The chemical parameters used for determining the components for PCA as well as spatial mixing patterns are the following: temperature, pH, conductivity, dissolved oxygen (DO), chloride (Cl^-), and sulfide (S_2). Other parameters with incomplete data were eliminated. These variables were selected based on available data for seven wells with the most complete analysis. One well, NDMW-15, was eliminated due to missing measurements for chloride. After the selections were identified the PCA analysis was performed on the selected six parameters to define the principal components and the associated eigenvectors to use in the EMMA analysis.

The variables with the greatest variance were then used in the end-member mixing analysis (EMMA). Using the available spreadsheet from the USGS (Christophersen and Hooper, 1992), the EMMA analysis was altered to fit the site parameters. EMMA confirmed the appropriate end-members selected, stream water and groundwater, and would be able to calculate

a percentage of each end-member and therefore subsequent percentages of mixing (Laaksoharju et al., 1999; Doctor et al., 2006; Valder et al., 2012) if the site fluids exist as mixtures of the end-member fluids. The chosen end-members for the analysis were selected from the USGS NWIS database and included the 1) Sacramento River, upstream of the field site, site number 11342000, and 2) water from a groundwater well, site number 411450122155301, located north-northwest of the field site within the river valley and the same watershed. USGS NWIS was used to evaluate regional end-members contributing to the water at the field site (United States Geological, 2014).

Lee et al. (2001) suggests using conservative solute tracers such as Cl^- and Br^- to identify areas of dilution and mixing. Previously measured chloride concentrations from the site were imported into ESRI ArcGIS and interpolated following the procedure listed under physical hydrogeology (ESRI, 2012). Additionally, site and regional chloride levels were compared, using the California groundwater monitoring system, Groundwater Ambient Monitoring and Assessment Program, GAMA, and the USGS National Water Information System (NWIS; United States Geological, 2014). Chloride was also analyzed against stream discharge measurements. Stream discharge data downloaded from the USGS NWIS Lakehead site, approximately 40 km (25 mi) south of the field site was plotted on a scatterplot with Cl^- concentrations for the site with corresponding dates. This comparison against stream discharge was also conducted for temperature, methane (CH_4), sulfide, and alkalinity.

NAPL TRANSPORT

For abiotic transport, standard methods to evaluation advection and migration are described. In order to indirectly determine the existence and characterization of the potential microbial populations at the field site a mechanism for NAPL migration, several proxies were used. These methods provide a basis for the role microbes play in the transport of NAPLs at this

field site and an understanding of the influence microbes have on dominating flow paths of NAPLs.

Advection

The horizontal groundwater velocity has been previously estimated based on historic measurements at this site. Additionally, Gentry et al. (2013) provided groundwater velocity estimates based from their groundwater flow model. The previously estimated velocities were compared to previous research to identify the roles of advection on the NAPL migration, as discussed by Sudsaeng et al. (2011).

Diving Plume

Characterizing a diving plume at the field site could allow for determining the primary mechanism of transport based on the previously discussed factors. This was completed by previous site reports that provided estimates of hydraulic conductivity across the site. Additionally, comparison was made with standard hydraulic conductivities based on lithology from Bear (1972). Hydraulic conductivities varying less than a factor of two would not be controlled by stratigraphic factors (Griesemer, 2001).

Data from the U.S. Climate Bureau was downloaded and averaged to create graph of local average monthly precipitation. This was used to provide estimates for recharge contributions to the field site, which would influence the diving rate of the plume (Weaver and Wilson, 2000; Nichols and Roth, 2006). To distinguish the amount of dispersion affecting a diving plume, Griesemer (2001) suggested identifying the zones of clean wells versus contaminated wells to map the plume.

Biological Factors

Using the ERSI ArcGIS database previously created, additional data were imported for the biological analysis. These datasets were imported and interpolated to a continuous surface (raster) from Topo to Raster within the 3D Analyst toolbox, including oxidation-reduction potentials (ORP), CH_4, S_2, carbon dioxide (CO_2), iron (Fe), sulfate (SO_4), DO, and alkalinity.

Previous samples of ORP and CO_2 were measured once, on July 21, 2011, in eight wells. Other chemical constituents, CH_4, S_2, and alkalinity were sampled previously from 13 wells over eight sample dates. Lee et al. (2001) used concentration contour maps of several chemical constituents, similar to Bennett et al. (1993), to determine the spatial pattern of the datasets. The significance of the patterns of individual chemical constituents can be extrapolated based on previous research. For example, elevated levels in CO_2 and HCO_3 from undergoing carbon oxidation processes as discussed by Fan et al. (2011) can suggests zone of biodegradation. Additionally, identifying areas of depleted solid Fe^{3+} and SO_4 and areas of additions of Fe^{2+} and S_2 suggest zones of biochemical processes. The types of biochemical processes were estimated based on standard values of ORP given from YSI, Inc. (2013) across the site. These were examined to indicate microbial reduction processes, e.g. iron reduction and/or sulfate reduction, related to biodegradation of NAPLs as discussed by Bennett et al (1993), Lee et al. (2001), and Fan et al. (2011). Additionally an increase in pH, alkalinity, and CH_4 will further support reduction as the one process of biodegradation (Lee et al., 2001; Fan et al., 2011). Other major metabolic products of biodegradation are carbonic and volatile organic acids, however there is not the appropriate field data to analyze these constituents (Atekwana et al., 2004).

The methods to examine the field site for biosurfactants are not available with currently available data; however, they are described by Banat (1995) and Walter et al (2010). Some chemical constituents can provide evidence of potential biosurfactant existence. Analyzing areas of high fluid conductivities would allow for interpretation of biosurfactant presence. Using previous ERI, zones of high bulk conductivity were noted spatially. Additional evidence

microbial activity can be determined from conductive ERI areas. If the ERI image shows areas of increased conductivity at the contaminated locations, based on Allen et al. (2007) and Atekwana et al. (2004a), then it may be that the increase in subsurface conductivity is from the dissolution of minerals and/or the addition of biofilms and conductive mineral phases, resulting from the biodegradation of NAPLs (Abdel et al., 2009). Further research needs to be conducted to better support where and if biosurfactants are present at our site as they are beyond the scope of this project.

CHAPTER VI

RESULTS

BASIC HYDROGEOLOGY

Geology

The influence of a permeability driven pathway caused from geologic gradients is difficult to discern in the gravel due to the homogeneity of the pathway with surrounding geology in the available data. The grain sizes within this zone consist mainly of gravels, boulders, and cobbles in a sandy silt matrix throughout the site. The gabbro and diorite bedrock are acting as a confining bed due to the substantial decrease in permeability based on hydraulic conductivity averages for these materials, approximately 10^{-8} m/s compared to the hydraulic conductivity of the alluvium, approximately 10^{-2} to 10^{-4} m/s. Additionally, the ERI images display the resistivity of the bedrock to be higher than the upper alluvial deposit (Figure 7). A geologic or stratigraphic preferential pathway for transporting NAPL is possible, but unknown due to the lack of a permeability data through the transporting gravel layer of subsurface at the site.

Physical Hydrogeology

The water table at the site dips to the S-SW direction (Figure 11). The highest potentiometric head at the field site is adjacent to the Sacramento River in the northeast corner with an elevation of 700 m (2,286 ft) above mean sea level. This elevated water table at the northern end of the site is due to the surface elevation difference from the northern to the southern

end of the site, approximately 6 m (20 ft). Five water level measurements were collected over a single year and show the evolution of the stream water input. June 2010 shows elevated water levels, which provides the first evidence that the site undergoes high stage flows that flood the subsurface of the site and create a periodic rising-falling water table. The eleven wells that were measured for water level produced show a water level gradient over the field site that is substantial for groundwater, as much as 0.015 m/m. The water level differences can vary by up to 4 m (13 ft) from the NE to SW and are supported by Gentry et al. groundwater flow model (2013; Figure 11). These water levels during flood conditions create a steep hydraulic gradient and a favorable condition for transport of water and hydrocarbons.

A graph of local monthly average precipitation shows the months with the highest average precipitation: December and January (Figure 12). However, in December the water table has a lower elevation than the other measured dates as the majority of this precipitation is in the form of snow. March has the highest averages for rainfall and subsequently one of the highest water table elevations. This provides further evidence of a system with a periodic rising and falling water table produced changes in the hydrologic conditions from high stage flow to baseflow.

Additional results from the investigation of basic transport mechanisms showed evidence that suggested groundwater in the north central area of the field site yielded the highest groundwater temperatures ranging from 15^{o}C to 20^{o}C with the lowest temperature on the edges of the field site ranging from 7^{o}C to 17^{o}C (Figure 13). The higher ranges of temperatures were inconsistent with ranges of other regional groundwater temperatures, which were located on the USGS NWIS mapper database within the same Upper Sacramento River Watershed (Figure 1; United States Geological, 2014). The regional groundwater and stream water temperatures are much lower than site temperature measurements (Table 1). Regional groundwater temperatures range from 8 to 13°C and stream water ranges from 6 to 15°C. Regional stream water temperature shows seasonal

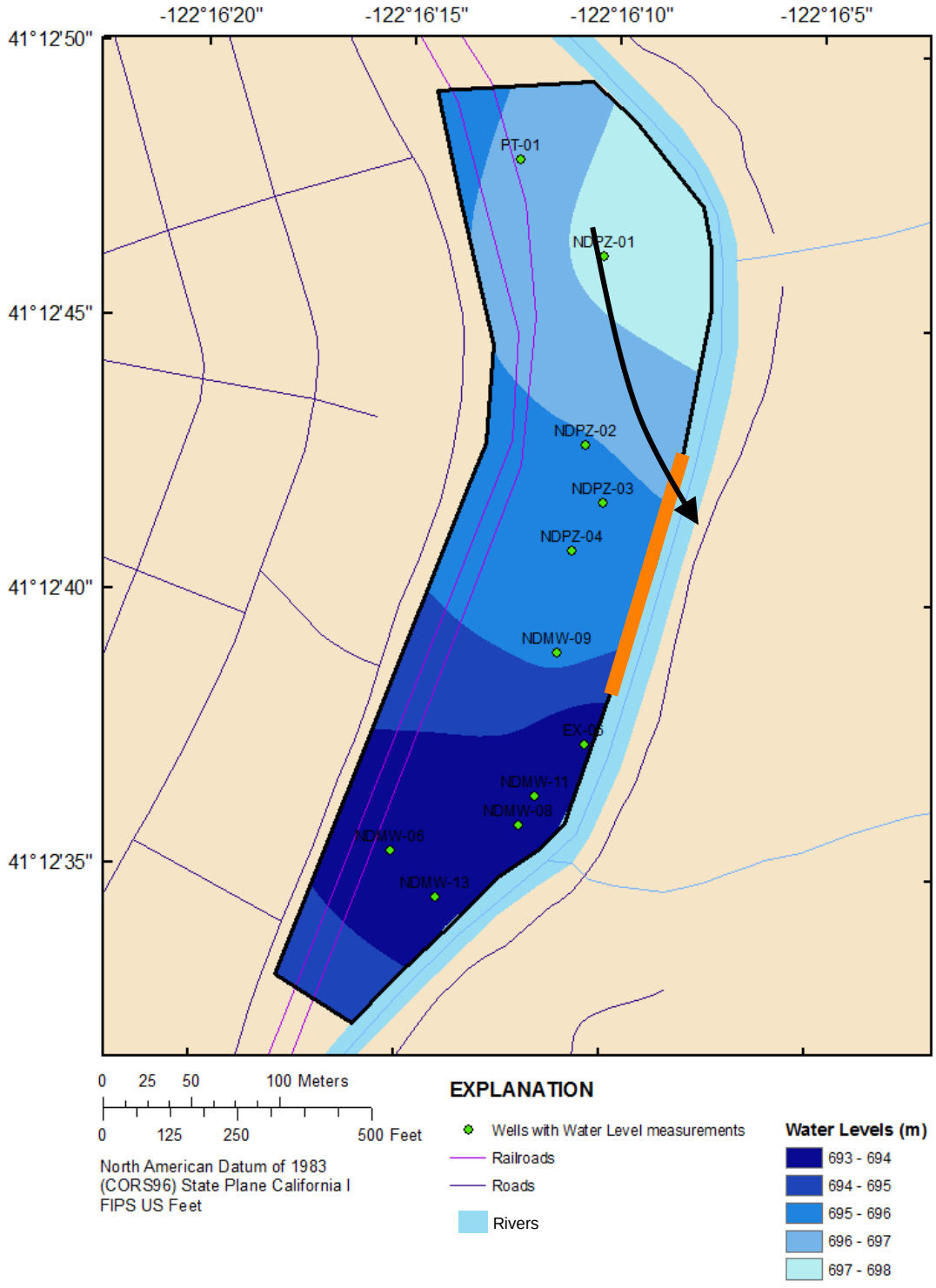

Figure 11. Maps showing the water table elevation at the field site in meters above mean sea level recorded June of 2010. Black arrow depicts the approximate location of the active NAPL migration pathway observed in Figure 7 data, orange line indicates 450' segment with NAPL seeps.

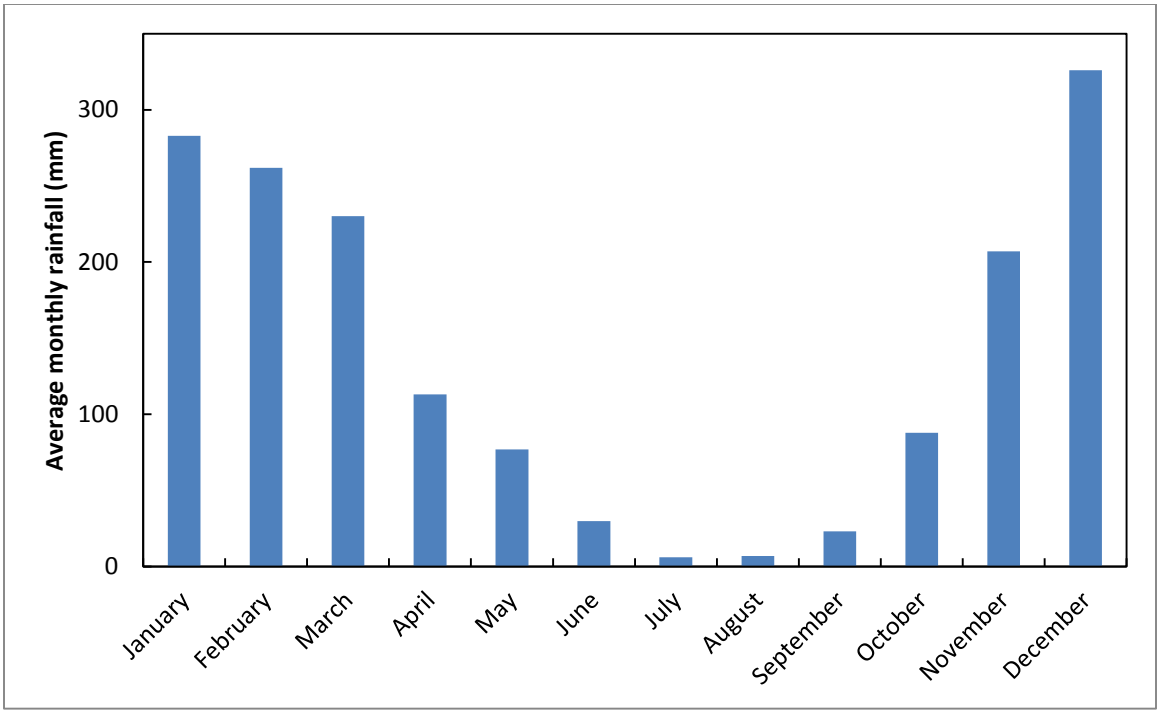

Figure 12. Graph showing the average monthly rainfall for Dunsmuir, CA in millimeters over the last 15 years.

variation greater than the regional groundwater. A graph of three site monitoring well temperatures compared to adjacent stream temperature illustrate that the site temperature variability differs from the regional temperature data (Figure 14). Monitoring wells reach temperatures ranges above the recorded local stream water temperature and of regional stream water and groundwater temperatures, which provides evidence that the heat source is being generated by in situ processes rather than input from a thermal source. The site wells with the highest temperature were not part of the continuously monitored dataset and are expected to have even higher difference in temperature compared with regional stream or groundwater.

The temperature trend mirrored the seasonal water table. The highest water table elevations matched the months with the lowest temperatures, supporting that the site undergoes pulse events that flood the site and lower overall site temperatures (Figure 13b). High temperatures within the field site correspond with lower overall stream discharge (Figure A-1 in

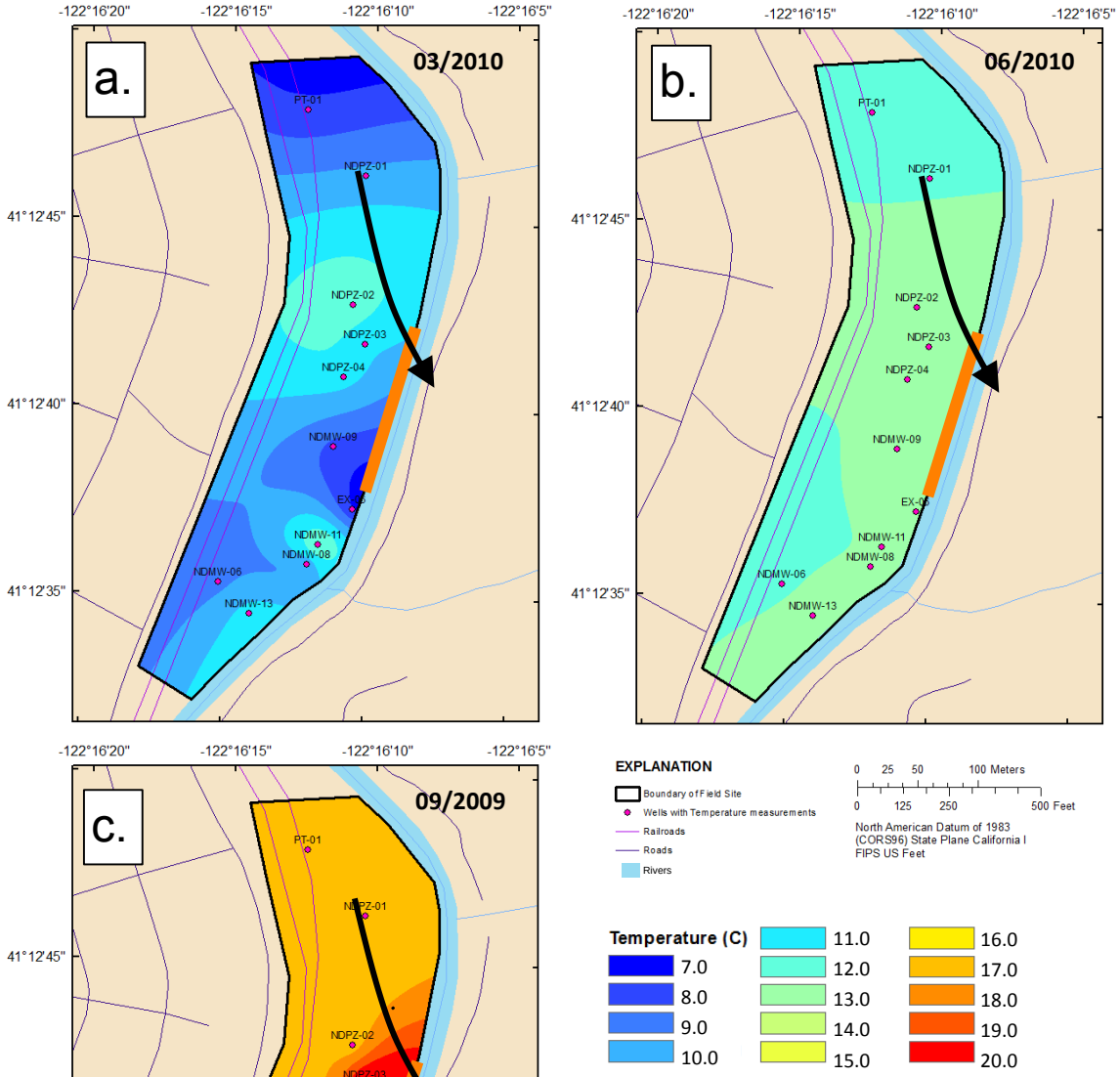

Figure 13. Maps showing the seasonal groundwater temperature in °C. June 2010 shows a period during high stage flows. March 2010 and September 2009 show periods during baseflow of varying seasonal temperatures. The highest temperatures are located in the north central area of the site boundary above the temperature of the stream. Black arrow depicts the approximate location of the NAPL migration pathway from Figure 6 data, orange line indicates 450' segment with NAPL seeps.

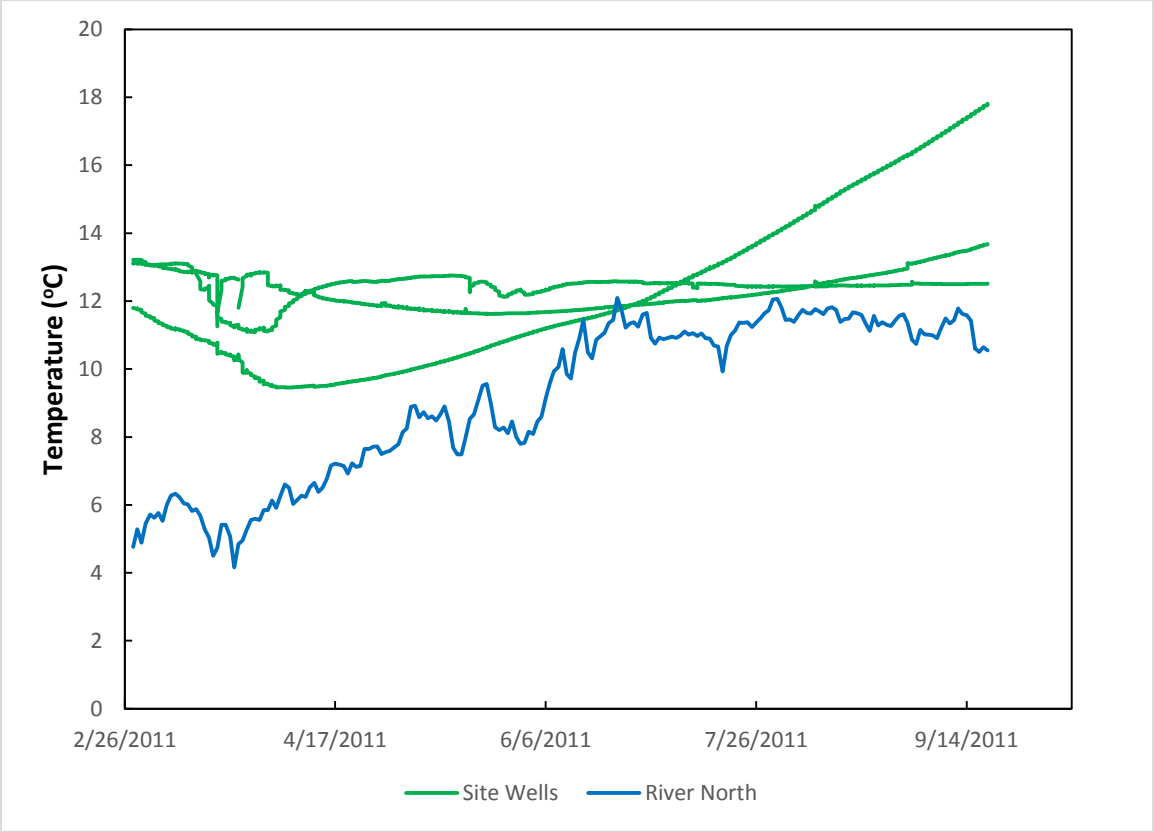

Figure 14. Graph showing the temperature in °C of three monitoring wells at the field site (MWX-02, NDMW-11, and SP-04), and the river temperature at the northern end of the site for the period of February to September of 2011.

Appendix). During baseflow, water levels decreased and many of the geochemical constituents increase, including CH_4, S_2, alkalinity, pH. Within the Upper Sacramento River Watershed, the regional groundwater pH remains relatively constant ranging from 6 to 7 and the regional stream water pH ranges from 7 to 8 (Table 1; Figure 15). This corresponds to the field site pH measurements for the southern end with the majority of the field site being slightly acidic with pH values of 6.25 to 7.75 (Figure 16). However, several well measurements, NDMW-14, NDMW-18, and NDMW-15, are anomalously high with pH values over 9, indicating potential biologic mechanisms. The uptake of acids by microorganisms for methane production can increase the pH (Segers, 1998). Across the regions pH values are less than 8, which correlate to

Table 1. Table showing the geochemistry of site groundwater, regional groundwater, and regional stream water.

	Well ID	Sample Date	pH	Temp	Conductivity	DO	Cl	S_2	SO_4
			(SU)	(°C)	(µS/cm)	(%)	(mg/L)	(mg/L)	(mg/L)
Site Groundwater									
	NDMW-14	7/21/2011	9.9	14.5	3713.0	0.0	430.0	17.0	17.0
	NDMW-15	7/21/2011	10.0	13.7	2689.0	0.2	-	15.0	-
	NDMW-16	7/21/2011	7.0	17.5	283.0	0.2	13.0	1.6	11.0
	NDMW-17	7/21/2011	7.8	15.5	327.0	0.1	11.0	1.0	4.2
	NDMW-18	7/21/2011	10.2	13.4	1744.0	0.0	89.0	1.0	3.9
	SP-04S	7/21/2011	6.5	14.1	337.0	75.2	20.0	1.0	11.0
	MWX-02S	7/21/2011	6.4	14.3	370.0	0.0	6.0	1.0	4.1
	NDMW-11S	7/21/2011	6.3	14.6	747.0	0.2	6.1	2.8	1.1
Regional Groundwater									
	411622000000000	9/16/1981	6.2	10.0	88.0	-	0.6	-	5.0
	411653000000000	2/16/1972	6.3	9.0	85.0	-	0.2	-	1.4
	411900000000000	7/15/2010	6.5	9.0	99.0	91.0	1.1	-	0.3
	411903000000000	9/16/1981	6.9	12.5	116.0	-	2.1	-	5.0
	412225000000000	9/16/1981	6.2	8.5	72.0	-	0.7	-	5.0
Regional Stream Water									
	11341440	3/23/1971	7.3	6.0	111.0	100.0	-	-	-
	11341400	8/26/1970	8.3	15.0	131.0	103.0	0.0	-	-
	11341365	11/11/1970	8.0	10.5	121.0	99.0	0.0	-	-
	11341344	8/27/1970	7.6	10.5	106.0	103.0	-	-	-
	11341342	8/27/1970	7.3	8.0	99.0	96.0	-	-	-

	Well ID	Sample Date	Fe	CH_4	NO_3	CO_2	Alkalinity	TOC
			(mg/L)	(mg/L)	(mg/L)	(mg/L)	(mg/L)	(mg/L)
Site Groundwater								
	NDMW-14	7/21/2011	1.0	2.8	1.0	0.2	580.0	4.8
	NDMW-15	7/21/2011		3.2	-	0.2	860.0	2.9
	NDMW-16	7/21/2011	3.7	0.2	1.0	-	75.0	1.4
	NDMW-17	7/21/2011	0.7	0.4	1.0	-	130.0	1.8
	NDMW-18	7/21/2011	11.0	0.4	1.0	29.0	190.0	2.4
	SP-04S	7/21/2011	0.2	0.0	1.0	23.0	99.0	1.0
	MWX-02S	7/21/2011	0.6	0.0	1.0	-	110.0	4.2
	NDMW-11S	7/21/2011	2.3	0.0	1.0	-	110.0	2.4
Regional Groundwater								
	411622000000000	9/16/1981	-	-	-	54.0	-	1.2
	411653000000000	2/16/1972	0.0	-	-	42.0	52.0	-
	411900000000000	7/15/2010	-	-	0.2	30.0	52.6	-
	411903000000000	9/16/1981	-	-	-	13.0	-	2.3
	412225000000000	9/16/1981	-	-	-	38.0	-	3.6
Regional Stream Water								
	11341440	3/23/1971	-	-	0.1	-	-	-
	11341400	8/26/1970	-	-	0.1	-	-	-
	11341365	11/11/1970	-	-	0.1	-	-	-
	11341344	8/27/1970	-	-	0.2	-	-	-
	11341342	8/27/1970	-	-	0.2	-	-	-

the pH values at the southern end of the field site. This provides evidence to support a background water source into the southern end of the site.

Groundwater Mixing

Initial chemical constituent values input for the PCA are shown in Table 2. The results of the PCA analysis include the six principal components and the cumulative variance of each one (Table 3). The EMMA analysis ideally provides the percentage of mixing of the selected end-members at the field site (Table 4). However, the regional groundwater and surface water end-members were closer in compositions than the variability across the site, allowing a comparison of site water against background waters, but not allowing an evaluation of mixing percentages. Many of the wells had similar composition to the regional waters, but several of the wells were major outliers and did not correspond well to either end-members, specifically, well NDMW-18 and NDMW-14, which are located at the northern end of the field site and have elevated parameters for pH, conductivity, and Cl (Figure 17; Table 2). NDMW-14 also has highly elevated S_2 concentrations. One well, NDMW-16, strongly correlated with the end-members, located in the center of the site, showed the least variability between parameters from the end-members to the wells. The other wells strongly correlate on the U1 plane and vary on the U2 plane, suggesting the end-members and site parameters are more closely related with the first principal component (U1) than the second (U2; Figure 17). After the EMMA analysis was conducted it is evident there is additional sourcing or reactions affecting the geochemistry at the northern end of the site. The two end-members did not fully produce an environment that could explain the mixing at the field site with the given water inputs, therefore additionally methods to determine the amount of mixing must be employed.

Although EMMA did not explain the percentage of each water mixing at the site, it did provide strong evidence that the site is altered at the northern end of the site and creates a geochemical environment much different from the source waters (Figure 18). A simple

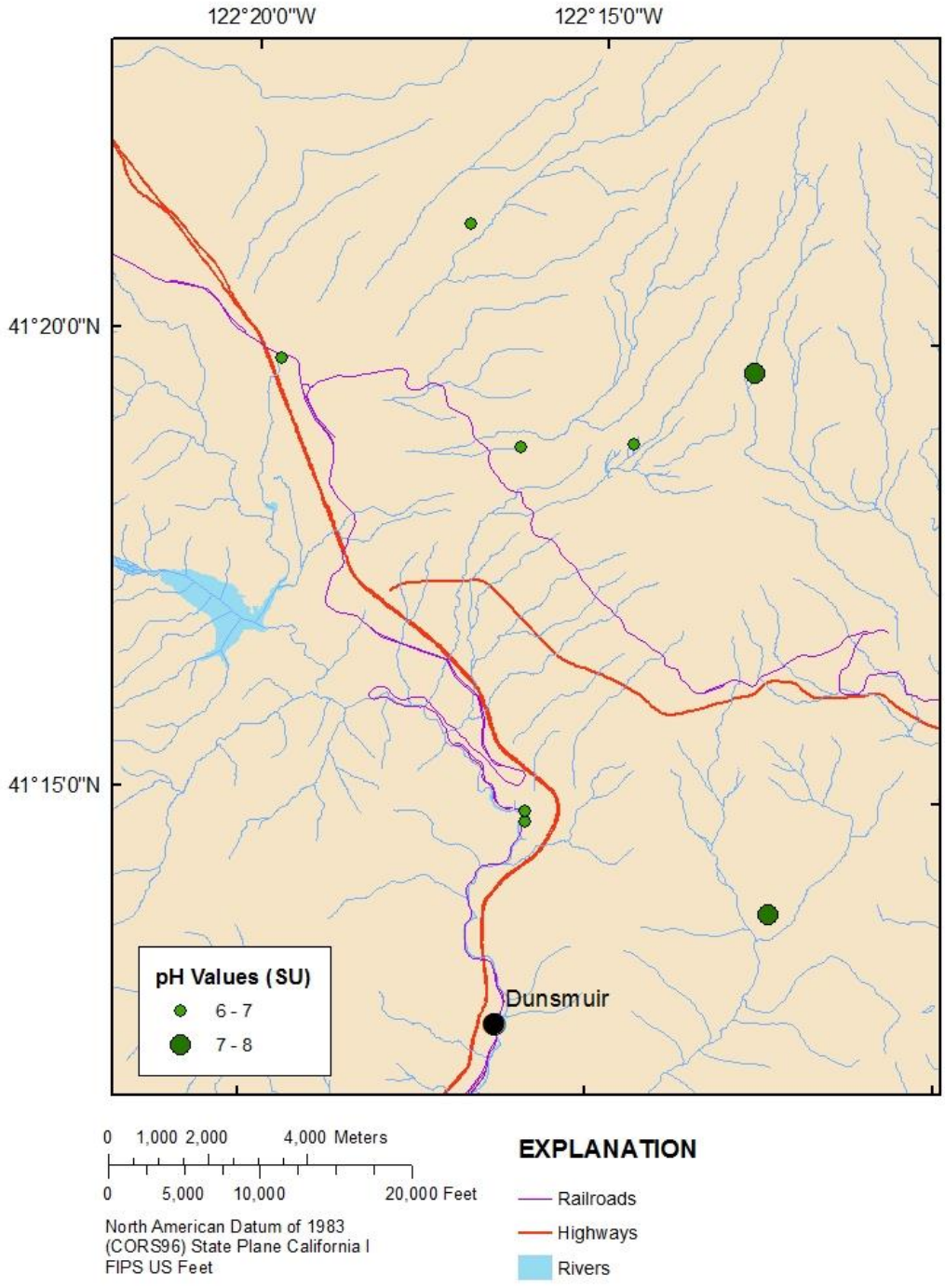

Figure 15. Map showing the pH values of the regional springs within the Upper Sacramento River watershed from the available data on the USGS NWIS.

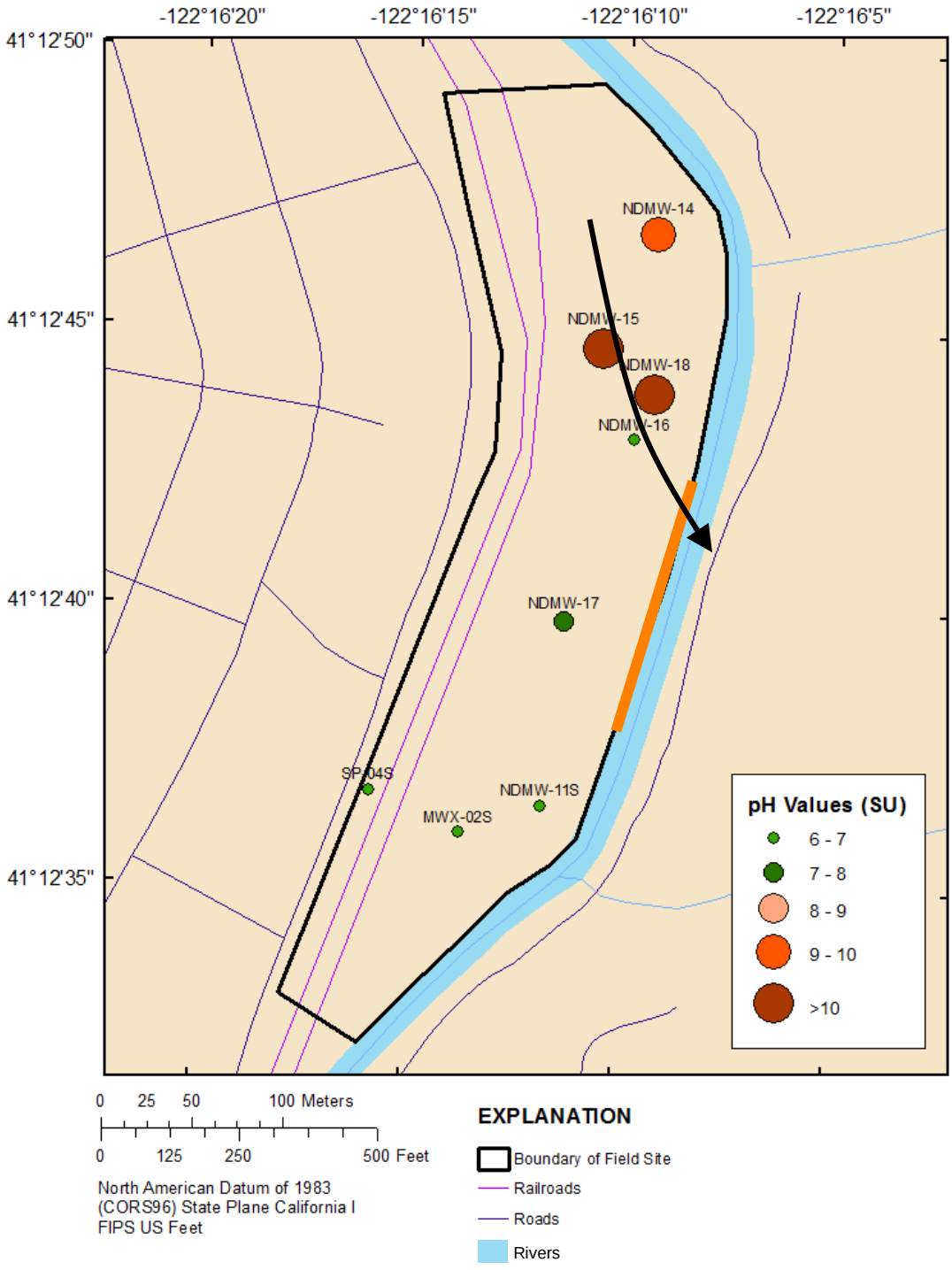

Figure 16. Map showing the pH in standard units of the field site. pH values <8.0 are shown in green and pH values >8.0 are shown in orange.

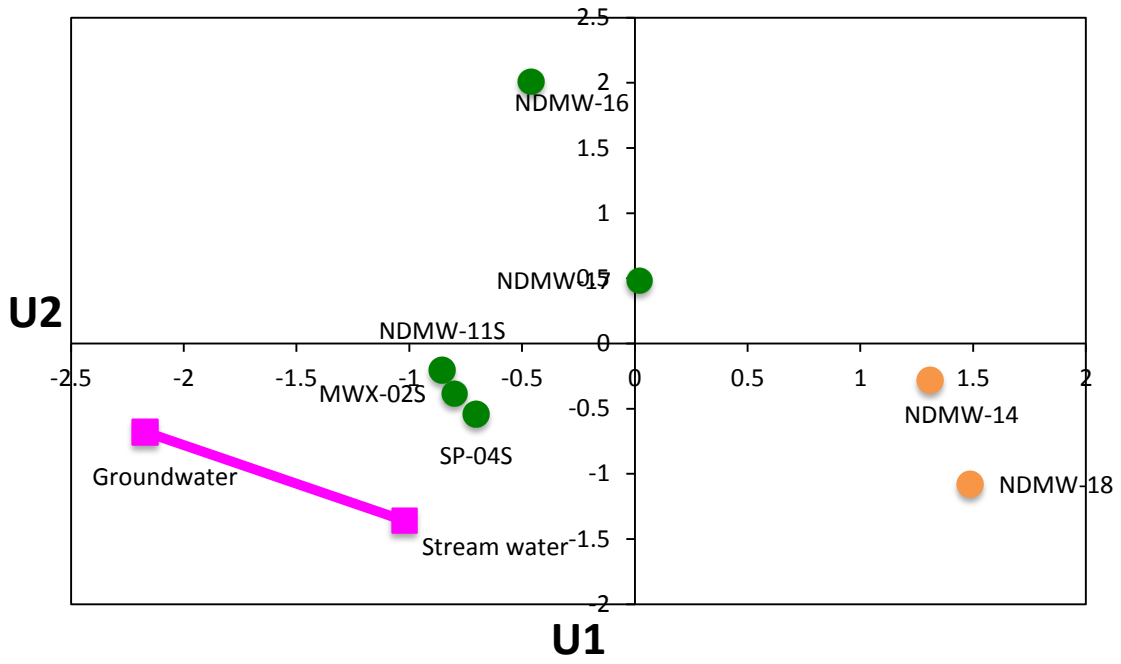

Figure 17. U-Space mixing diagram showing the degree of variability in the wells compared to the two end-members, the stream water and groundwater.

comparison of Table 2 and Table 4 provides evidence that the well geochemistry at the field site lies outside the range of the source waters. Limited areas of the field site have extreme geochemical outliers, such as pH in the northeast corner, suggesting the area of strongest in situ reactions. Additionally, conductivity showed the highest loading for the dataset. To determine the next most influential parameter on the dataset, conductivity was altered to a single concentration for all wells. Chloride showed the highest loading after this alteration. This was done for all parameter to gain a better understanding of the order of influence each parameter had on the PCA and EMMA analyses. The order was from most influential parameter to least; conductivity, Cl, DO, S_2, pH, temperature.

Interference from onsite reactions or other anthropogenic effects limits the ability to distinguish the percentages of the source waters entering the site through geochemical and statistical analyses. However, a conservative tracer can be used to determine the dominant mixing

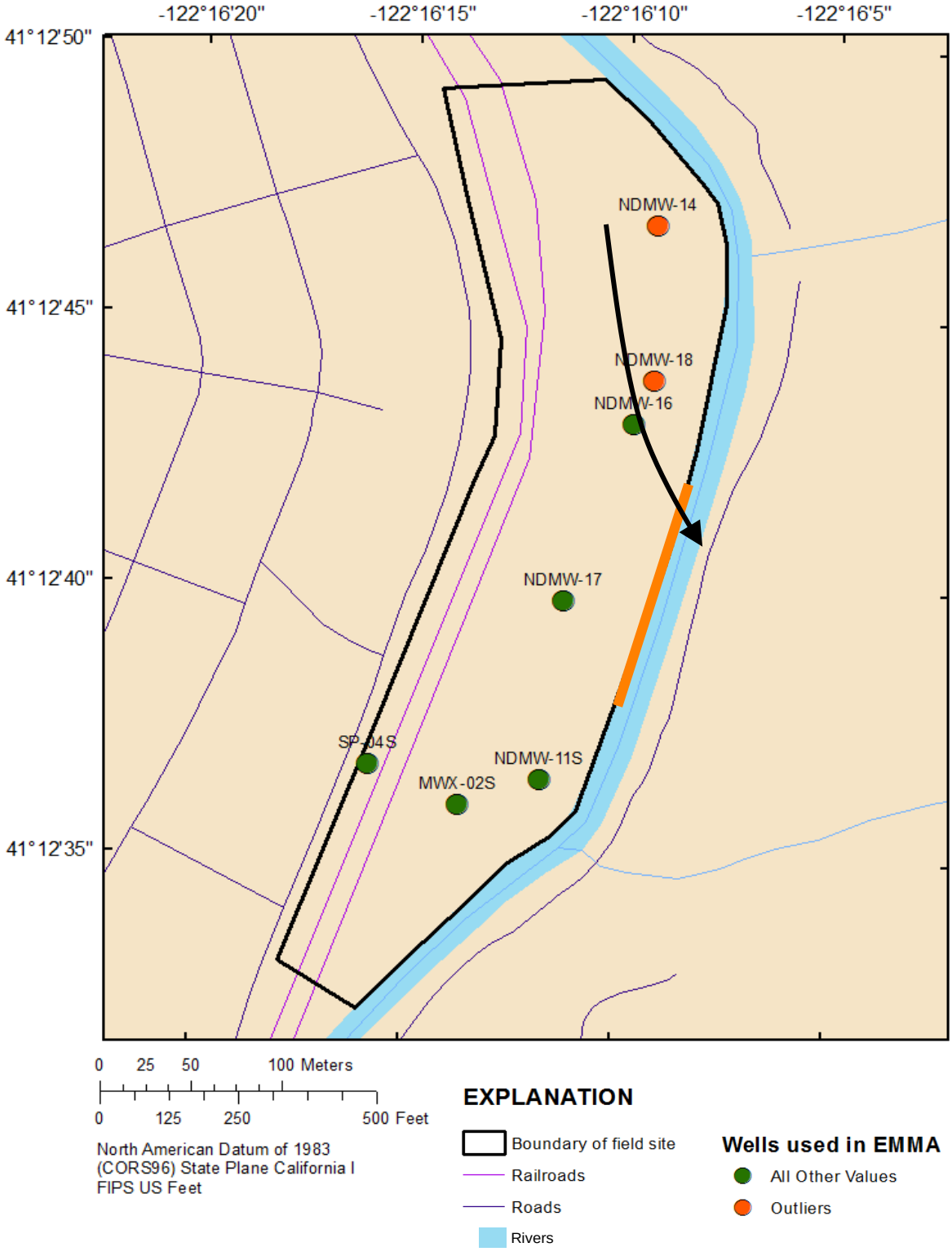

Figure 18. Map showing the distribution of wells analyzed in PCA and EMMA corresponding to Figure 17, U-Space Mixing diagram.

pattern at the site. The results from investigating the available conservative solute tracer, Cl, show support for dilution and a dominant mixing pattern at the field site, specifically related to the influence of flooding the subsurface from high stage flow (Figure 19). The eighteen wells analyzed for Cl at the field site range from less than 1.0 to greater than 100.0 mg/L over two years of monitoring with September 2011 having the highest recorded values. A graph of total monthly precipitation is shown for 2011, 2012, and 2013 (Figure 20). The months with the highest precipitation, specifically March 2012, correlate to less variability in the Cl amounts across the field site, indicative of dilution and mixing supporting that the site undergoes high stage flows that flood the site (Figure 21).

The stream discharge data from the Sacramento River shows high variability of flow over approximately two years of data. The range of flows are from less than 200 cfs to greater than 13,000 cfs. Additionally, the Sacramento River discharge data further suggests high stream flow correlating with less variable Cl data. When comparing stream discharge of the Sacramento River against a monitoring well in the northern end of the field site, NDMW-14, an exponential fit to the data has a high coefficient of determination (R^2), ~0.97, for chemical constituents supporting the interpretation of high stage flows flushing the site. Appendix A contains graphs of other chemical constituents compared to stream discharge with high correlation relative to geochemistry of the constituents used in the mixing analysis.

Further investigation of the regional Cl concentration suggests the Cl concentrations at the field site are substantially greater than the groundwater and stream water in the region, dismissing natural volcanic sources as the Cl input (Table 1). Locally, groundwater wells slightly northwest of the field site show elevated Cl concentrations similarly to the field site. Additional Cl is suspected of being added to the groundwater via recharge through anthropogenic sources

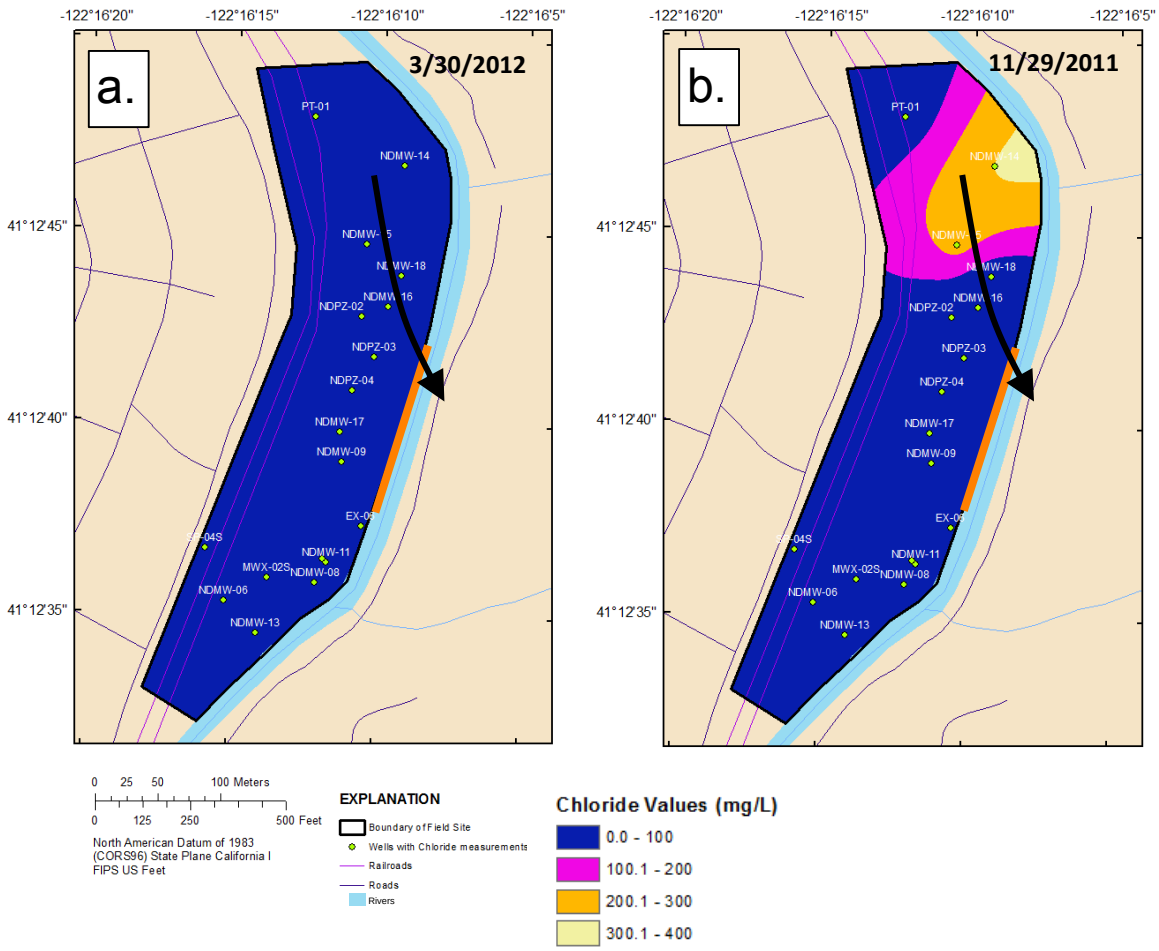

Figure 19. Maps showing the evolution of Cl values in mg/L during high stage flows (left; 19a) to baseflow (right; 19b). Black arrow indicates the transport pathway, orange line indicates 450' segment with NAPL seeps.

(e.g. deicing salts at the rail yard; Mullaney et al., 2009). The spatial and temporal distribution of Cl values provides strong support for a system that is periodically flooded from high stage flows. When Cl levels are consistent across the field site, the system is being dominated by high stage surface water flows. However, when the site is experiencing baseflow, it is being dominated by slow input at the northern end of the site seen from the slow increase of Cl after a high stage flow and consistent input from groundwater at the southern end of the site, reflected by the consistency

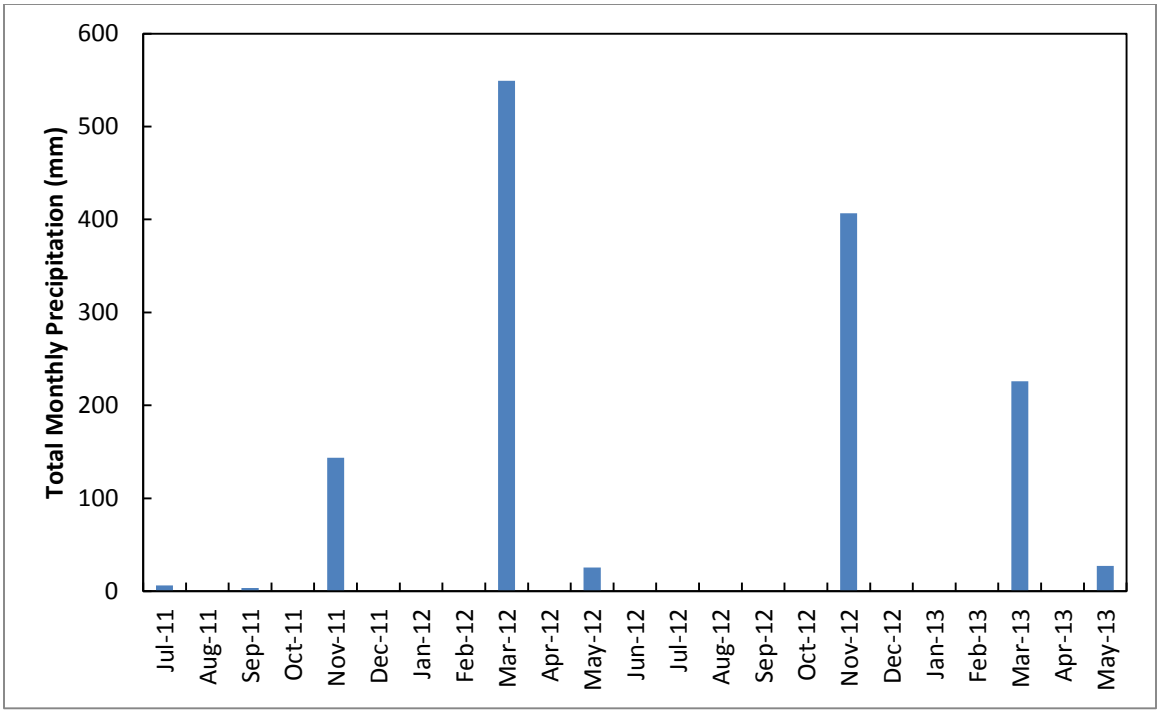

Figure 20. Graph showing the total monthly precipitation from July 2011 to May 2013 for Dunsmuir, CA in millimeters.

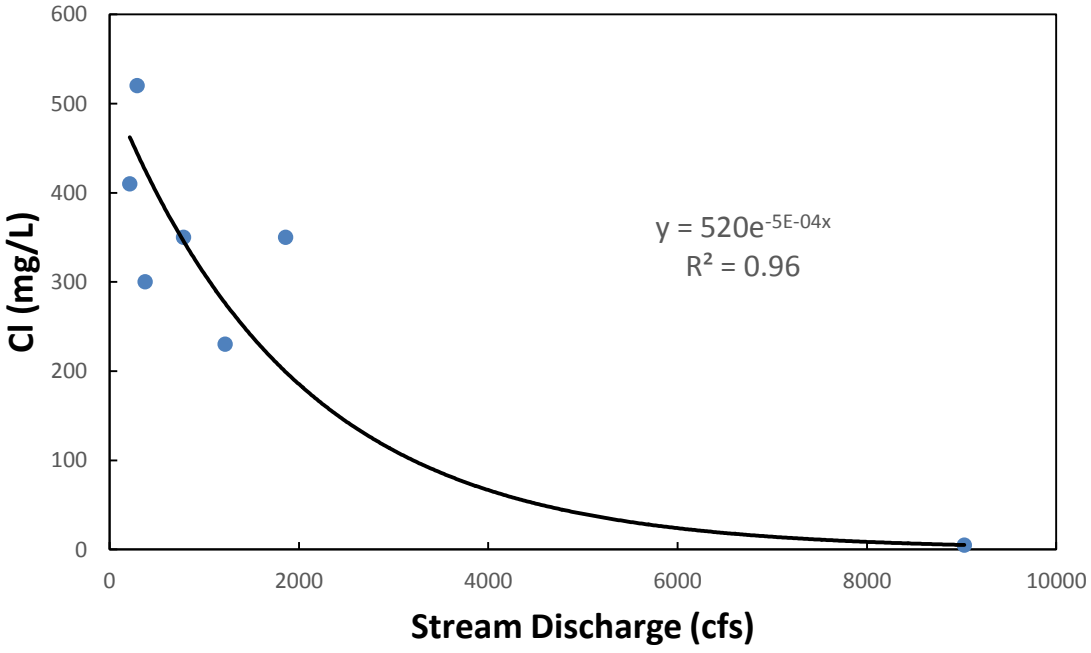

Figure 21. Graph showing the daily discharge of the Sacramento River approximately 40 km (25 mi) south of the field site at the Lakehead location with Cl measurements from a well in the northern area of the field site, NDMW-14.

Table 2. Chemical parameter input from the field site used for the PCA/EMMA.

		Water Quality Parameters					
	Sample Date	Temperature	Conductivity	pH	Cl	DO	S_2
		(°C)	(µS/cm)	(SU)	(mg/L)	(%)	(mg/L)
NDMW-14	7/21/11	14.5	3713.0	9.9	430.0	0.0	17.0
NDMW-16	7/21/11	17.5	2689.0	7.0	13.0	0.2	1.6
NDMW-17	7/21/11	15.5	283.0	7.8	11.0	0.1	1.0
NDMW-18	7/21/11	13.4	327.0	10.2	89.0	0.0	1.0
SP-04S	7/21/11	14.1	1744.0	6.5	20.0	75.2	1.0
MWX-02S	7/21/11	14.3	337.0	6.4	6.0	0.0	1.0
NDMW-11S	7/21/11	14.6	370.0	6.3	6.1	0.2	2.8

Table 3. Results of the PCA from six monitoring wells from July 21, 2011 showing the principal components of the dataset (PC) and the cumulative variance of the principal components.

Variable	**Temperature**	**Conductivity**	**pH**	**Cl**	**DO**	**S_2**	**Cumulative Variance**
PC1	-0.023	0.982	0.096	0.012	-0.03	0.159	0.974
PC2	-0.225	0.022	-0.224	0.009	0.938	0.138	0.987
PC3	-0.427	0.044	0.591	-0.02	0.136	-0.669	0.997
PC4	0.762	-0.04	0.564	0.02	0.307	0.072	1
PC5	0.432	0.179	-0.521	-0.057	0.079	-0.707	1
PC6	0.003	0	-0.028	0.998	-0.007	-0.058	1

Table 4. End-members for EMMA analysis.

End-member	**Temperature (°C)**	**Conductivity (µS/cm)**	**pH (SU)**	**Cl (mg/L)**	**DO (%)**	**S_2* (mg/L)**
Stream water	11.5	83.6	7.8	4.5	102.3	0.0
Groundwater	8.0	98.0	6.6	1.9	100.0	0.0

*S_2 was estimated based on saturated DO concentrations and standard ranges of sulfate values for the watershed.

between regional and site concentrations. The mixing of these waters has created unique characteristics for this site driven by the periodic flooding from high stage flows.

NAPL TRANSPORT

Advection

The previous recorded groundwater velocities are estimated at 2.2×10^{-4} m/s (2.7 ft/hr) from tracer tests. Further historic estimates report 1.4×10^{-4} to 2.8×10^{-4} m/s (1.5 to 3.4 ft/hr) for groundwater velocities across the field site. Gentry et al. (2013) performed a hydraulic analysis to estimate groundwater velocities through the primary flow path with ranges from 1.2×10^{-5} to 1.7×10^{-5} m/s (3.3 to 4.9 ft/day). Groundwater velocities up to 1.7×10^{-5} m/s (5 ft/day) are sufficient to mobilize NAPL; therefore the velocities within the system are capable of transporting mobile NAPLs (Gentry et al., 2013).

Diving Plume

Hydraulic conductivities were not calculated or measured for this site; however, estimates were made based on grain-size, materials, and previous determinations. The estimates of grain sizes correspond with the cross section (Figure 6; Bear, 1972). The transporting layer has estimated hydraulic conductivities of 10^{-2} to 10^{-4} m/s. Weaver and Wilson (2000) indicate areas with diving plumes exhibit increased hydraulic conductivities with depth, however due to the heterogeneity of the lithology through the transporting layer this is not an effective means for determining the existence of a diving plume. Additionally, the bedrock is acting as a confining unit with very low hydraulic conductivities. Identifying zones of clean wells and contaminated wells was not applicable at this field site due to the extent of contamination and the shallow aquifer depths. However, NAPL was identified below the water table in wells, NDMW-15, NDMW-16, and NDMW-18, as much as 2 m (7 ft) below the water table, indicating a diving plume.

The 2D ERI transect provides further evidence of a diving plume as the high conductivity pathway with below the water table (Figure 11). Additionally, the 12 wells located within the ERI conductive pathway were all found to have NAPL. The NAPL increased in depth with proximity to the concrete retaining wall and in some wells was over 2 m (7ft) below the water table (Figure 9). The significant amount of NAPL below the water table provides evidence of the movement of the NAPL plume downward.

Additionally, the site experiences several factors that support an environment suitable for diving plumes, such as higher water elevations from groundwater to surface water, high volume of waters moving through the site, and a time period of over 100 years (Weaver and Wilson, 2000; Griesemer, 2001; Nichols and Roth, 2006). The NAPLs present below the water table coupled with the properties of vertical dispersion are capable of creating a diving plume at the site that are able to move under the concrete retaining wall and into the stream.

Biological Factors

To evaluate the potential for biodegradation and to identify the most viable types of degradation, oxidation-reduction potentials (ORP) were evaluated. The YSI-determined ORP values associated with corresponding process are shown in Table 5. As Bennett et al. (1993) discussed a decrease in ORP values indicates a reducing environment. The ORP values transition from very negative in the northern end to slightly positive in the southern end (Figure 22). For example, on July 2011, well NDMW-14 in the northern end shows an ORP value of -202 mV compared to well SP-04S in the southern end with an ORP value of 145 mV. The differences in ORP could provide evidence of areas where background water is influencing the site verses in situ biochemical processes. The increase in ORP values at the southern end of the site is evidence of groundwater input at that end of the site as the regional groundwater is oxic. This can also be

supported by the dilution or mixing effect. The geochemical parameters at the southern end of the site have low fluctuations compared to the northern end of the site.

The northern area of the site is undergoing sulfide formation and methane production, supported by the ORP values ranging from -250 to -50 mV, as well as the increased CH_4 values, >2 mg/L (Figure 23), and S_2 values, >4 mg/L (Figure 24). Elevated S_2 concentrations indicate the areas where sulfate reduction is taking place and where microbial populations are most likely present. The northern part of the site has increased levels of S_2 (Figure 24). Well NDMW-15 shows elevated S_2 levels of 22 mg/L, located in the northern end of the site.

The elevated ORP values in the southwest correspond to increased levels in DO. One well in the southwest end of the site, SP-04S, shows elevated DO percent (>75%) and ORP values (>140 mV). The ORP range is indicating the site is experiencing biochemical oxygen demand (cBOD; oxidation of only carbons) degradation with free molecular oxygen (Table 5). The remaining wells at the site contained low amounts of DO, indicating an anoxic environment.

The field data were reported in percent. The vast majority of the field site falls below 20% DO concentrations. DO reaches 100% saturation at approximately 8.0 mg/L at 25°C, therefore 20% DO is approximately 1.6 mg/L DO (United States Geological, 2014). The lowest saturation is in present in wells SP-04S and NDMW-18. Both wells with elevated CO_2 correspond to active oxidation-reduction processes, as listed above. Additionally, conductivity values are elevated in the northern end of the site in wells NDMW-14 (2.93 mS/cm) and NDMW-15 (2.08 mS/cm; Figure 26). The conductivity was sampled at a time of baseflow conditions.

The highest alkalinity concentrations are in the northern end of the site in wells NDMW-14 (610 mg/L) and NDMW-15 (620 mg/L; Figure 27). Minor elevated concentrations are observed seasonally at the southwest end in well NDMW-06 (470 mg/L). Due to the relationship of alkalinity and pH, the site exhibits higher pH values where elevated alkalinity values are present.

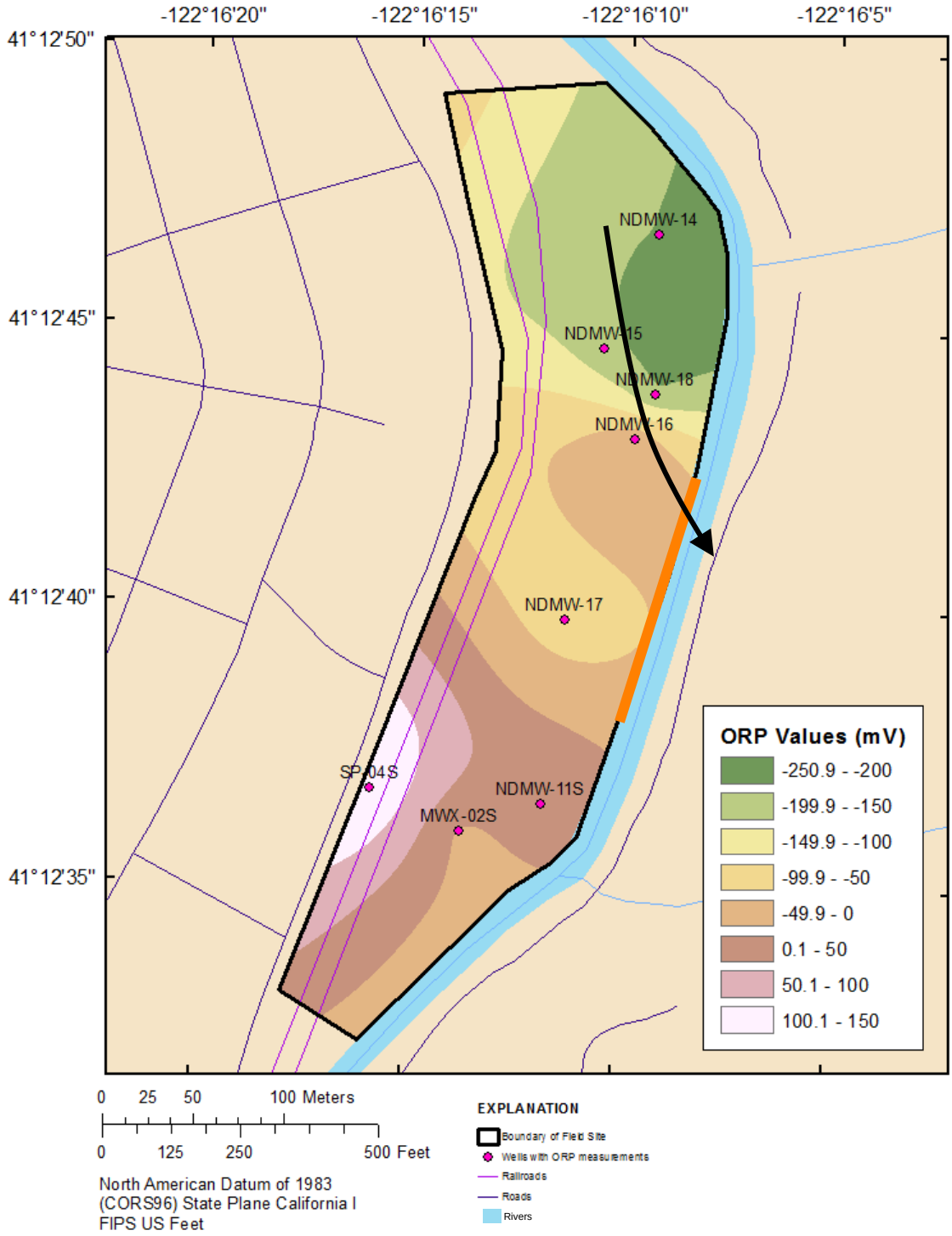

Figure 22. Map showing oxidation-reduction potentials (ORP) values in mV for July 21, 2011. The site values correspond to the ranges listed in Table 5 below. Black arrow indicates transport pathway, orange line indicates 450' segment of NAPL seeps.

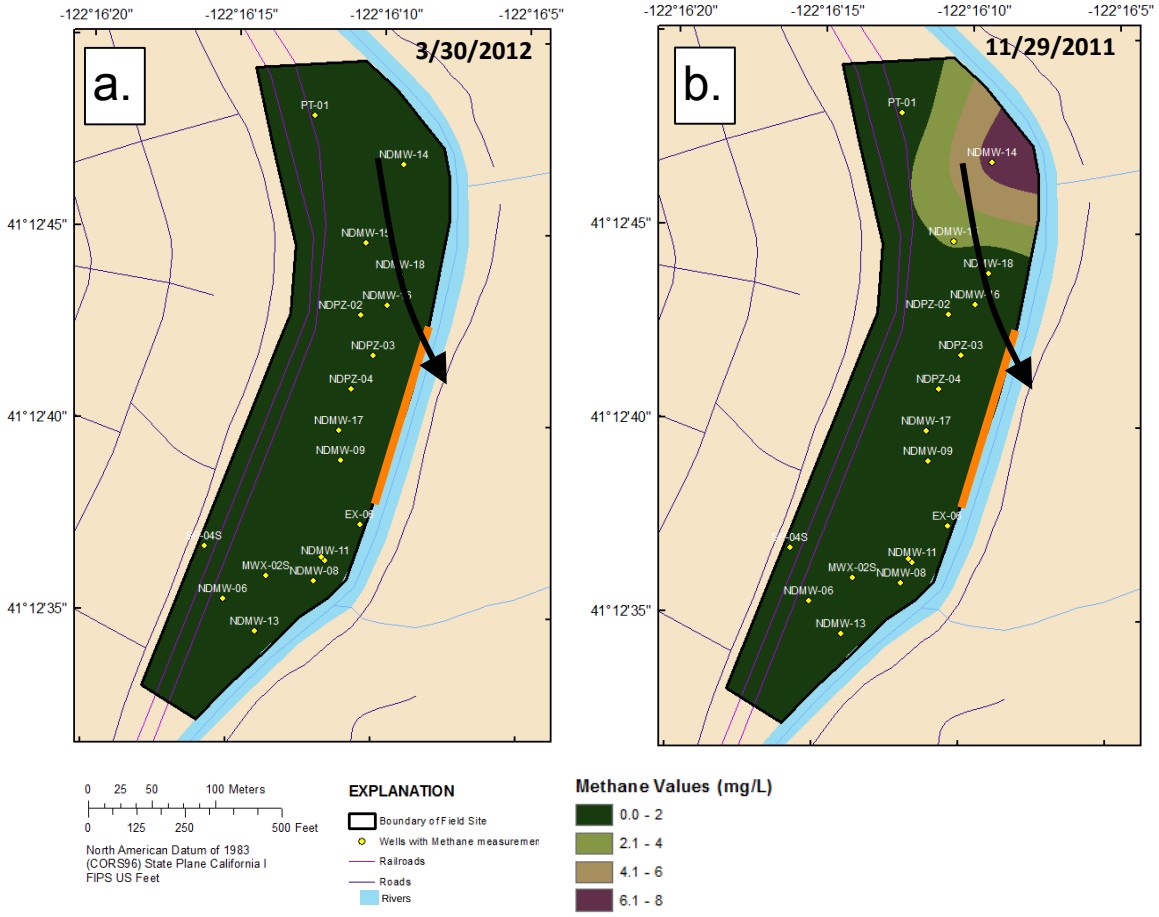

Figure 23. Map showing the CH_4 concentration in mg/L during high stage flows (left; 23a) vs. baseflow (right; 23b). Black arrow indicates transport pathway, orange line indicates 450' segment with NAPL seeps.

Table 5. Typical values of wastewater modified from YSI, 2013.

ORP (mV)	Process
-400 to -175	Methane production
-225 to -100	Acid formation (fermentation)
-250 to -100	Biological phosphorus release
-250 to -50	Sulfide (H_2S) formation
-50 to +50	Denitrification
+25 to +250	Biological phosphorus removal
+50 to +250	cBOD degradation with free molecular oxygen
+100 to +350	Nitrification

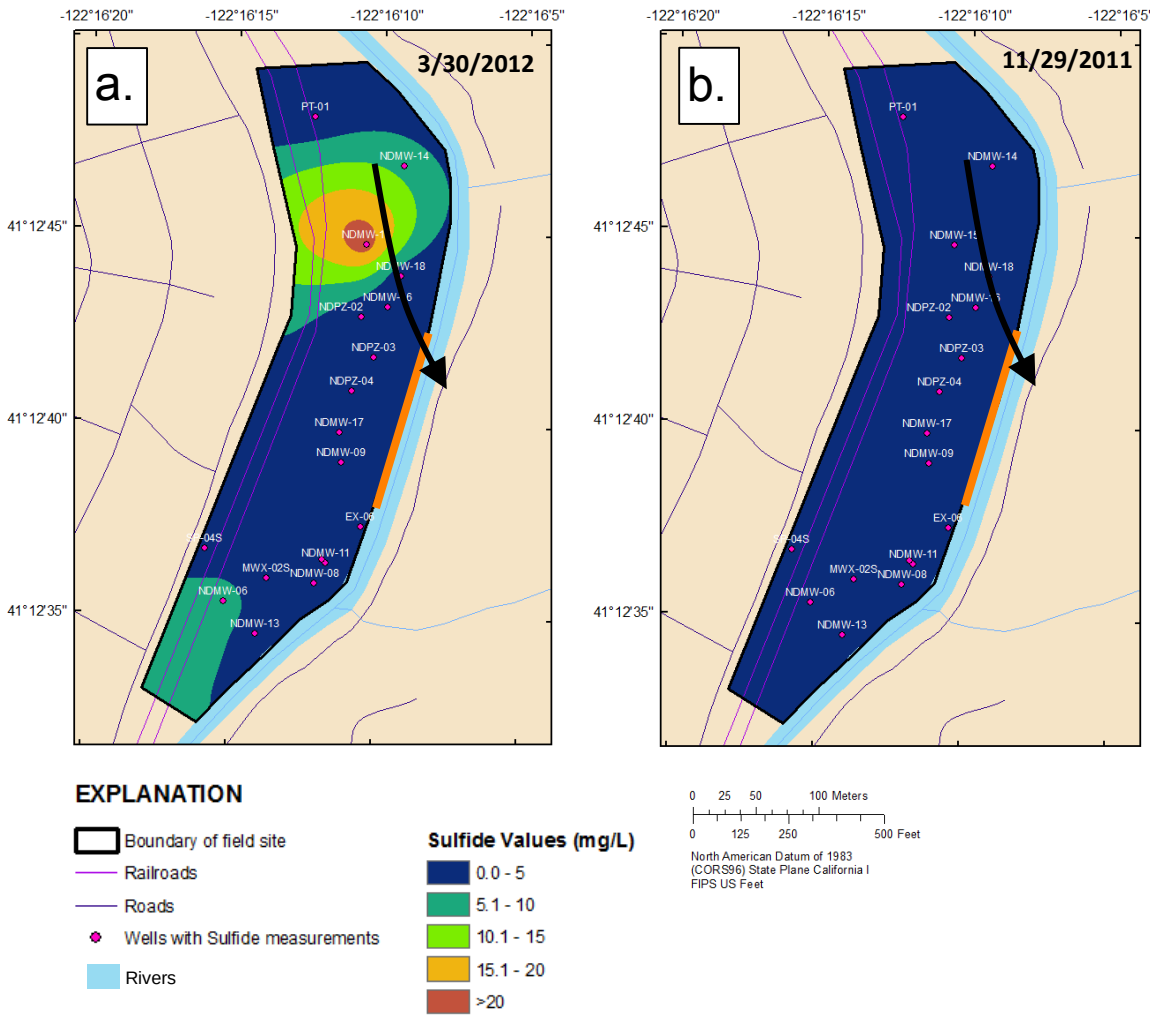

Figure 24. Map showing the S_2 concentration in mg/L during high stage flows (left; 24a) verses baseflow (right; 24b). Black arrow indicates transport pathway, orange line indicates 450' segment with NAPL seeps.

the northern end of the field site is from wells NDMW-14 indicating 0.0 % DO. The depleted DO indicates active areas of anaerobic degradation (Fan et al., 2011).

Based upon the hydro-geochemical analysis, the evidence for biochemical processes in the subsurface can be observed through concentrations of byproducts such as CO_2 and HCO_3. These help to identify areas where biological activities are undergoing. Fan et al. (2011) describes CO_2 as a usual initial product of biodegradation processes. CO_2 is highest in the northern and southwestern area of the field site at greater than 12 mg/L (Figure 25). The elevated CO_2 is

The pH values are increased at three northern well sites, NDMW-14, NDMW-15, and NDMW-18, with pH values of greater than 9.9 (Figure 16).

The locations of the elevated alkalinity concentrations coupled with pH provide further evidence to support biochemical processes at the field site. Additionally, CH_4, S_2, and alkalinity demonstrate the evolution from baseflow to high stage flow (Figures 23-24, 27). March 2012 corresponds to a high precipitation month reflected in the homogenization of the chemical constituents across the site. Further evidence of high stage flows correlating to the amount of chemical constituents is illustrated by comparisons of stream discharge and select chemical constituents (Appendix A). November 2011 corresponds to baseflow and the elevated concentrations are seen primarily in the northern end (Figure 27). Similar to most of the geochemical parameters investigated in this research, which demonstrates a system that experience periodic flow shifts from baseflow to high stage flow.

Sulfate, which is a reactant of redox reactions, can be used to estimate the extent and areas where biochemical reactions are occurring. Depleted levels of electron acceptors, such as DO or sulfate, provide evidence for the areas with the highest amount of biochemical processes occurring, such as methanogenesis or sulfate reduction (Atekwana et al., 2004; Cloutier et al., 2008). Therefore, the expectations of sulfate levels would be to decrease at the field site, however Lee et al. discusses newly supplied recharge water can introduce sulfate and nitrate back into the system (2001). Since sulfate levels in the regional stream water and groundwater are substantially lower than the field site this conclusion can be discounted (Table 1). Additionally, the field site does not experience complete dilution and homogenization of sulfate like the other geochemical constituents during high stage flow.

Understanding the evolution of several chemical constituents allows for extrapolation of the location of biodegradation, through the assumption that microbes are serving as the catalysis

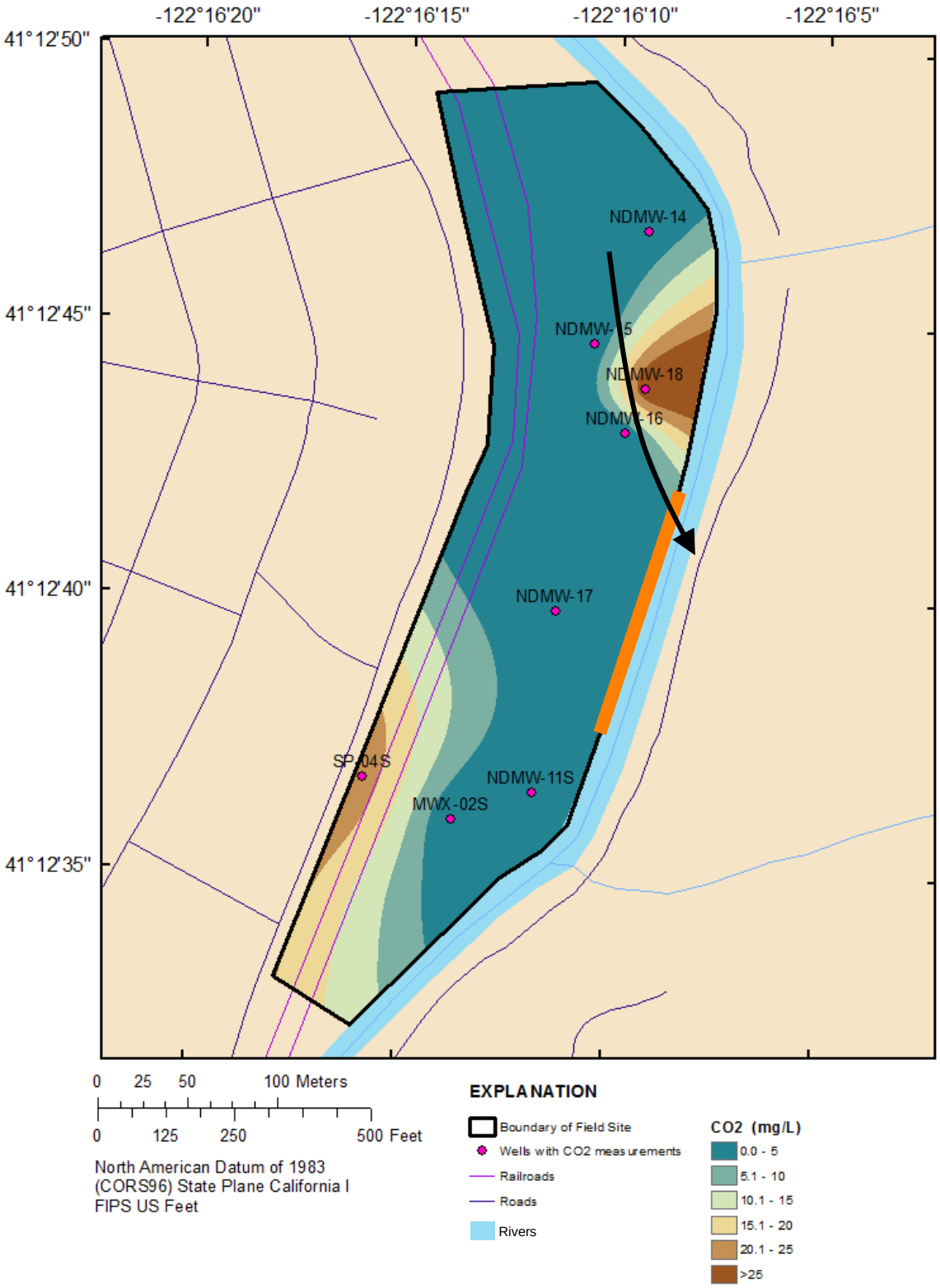

Figure 25. Map showing CO_2 concentrations in mg/L for July 21, 2011. Black arrow indicates transport pathway, orange line indicates 450' segment with NAPL seeps.

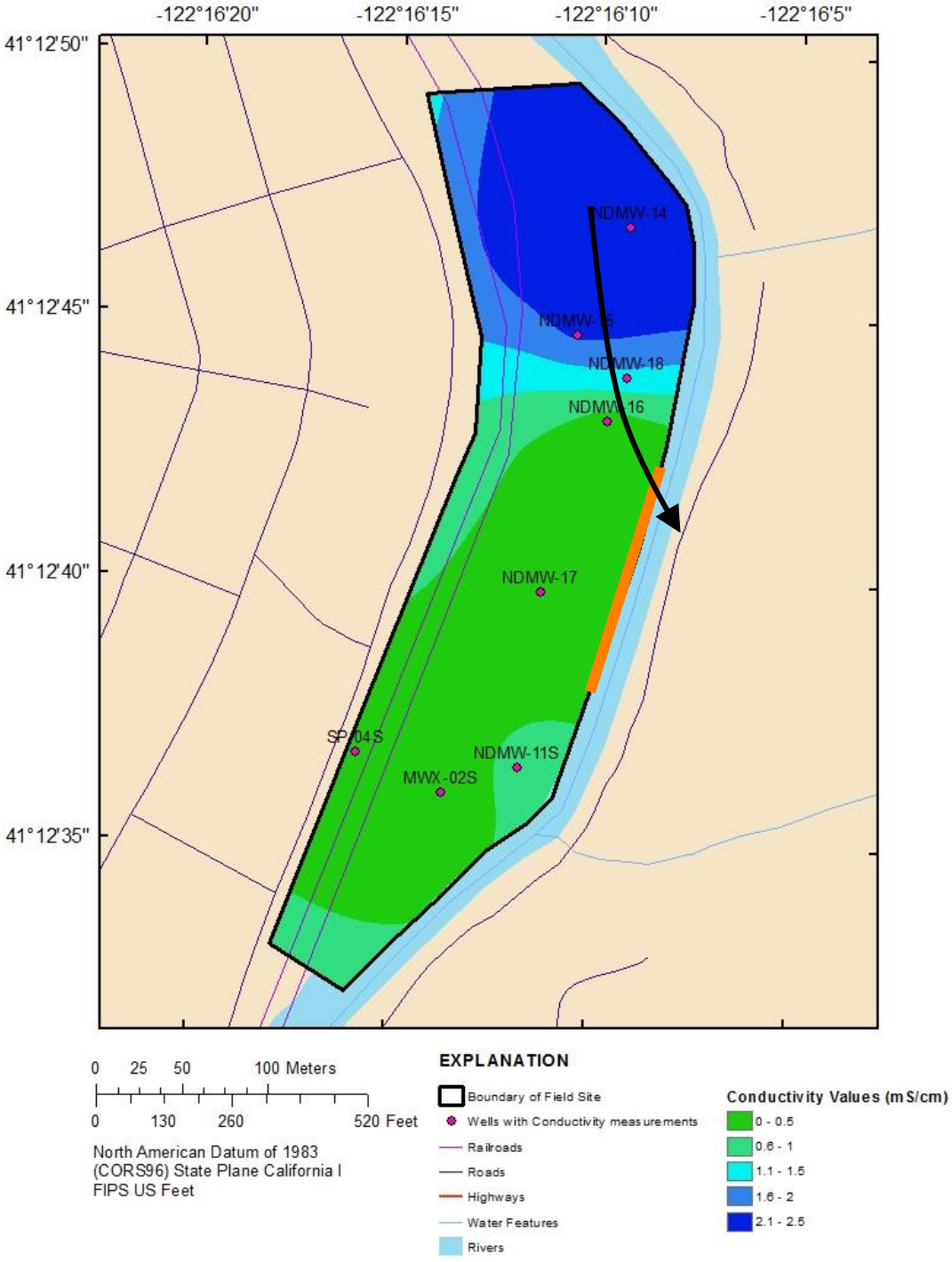

Figure 26. Map showing the conductivity values across the site in mS/cm for July 21, 2011. Black arrow indicates the transport pathway, orange line indicates the 450' segment with NAPL seeps.

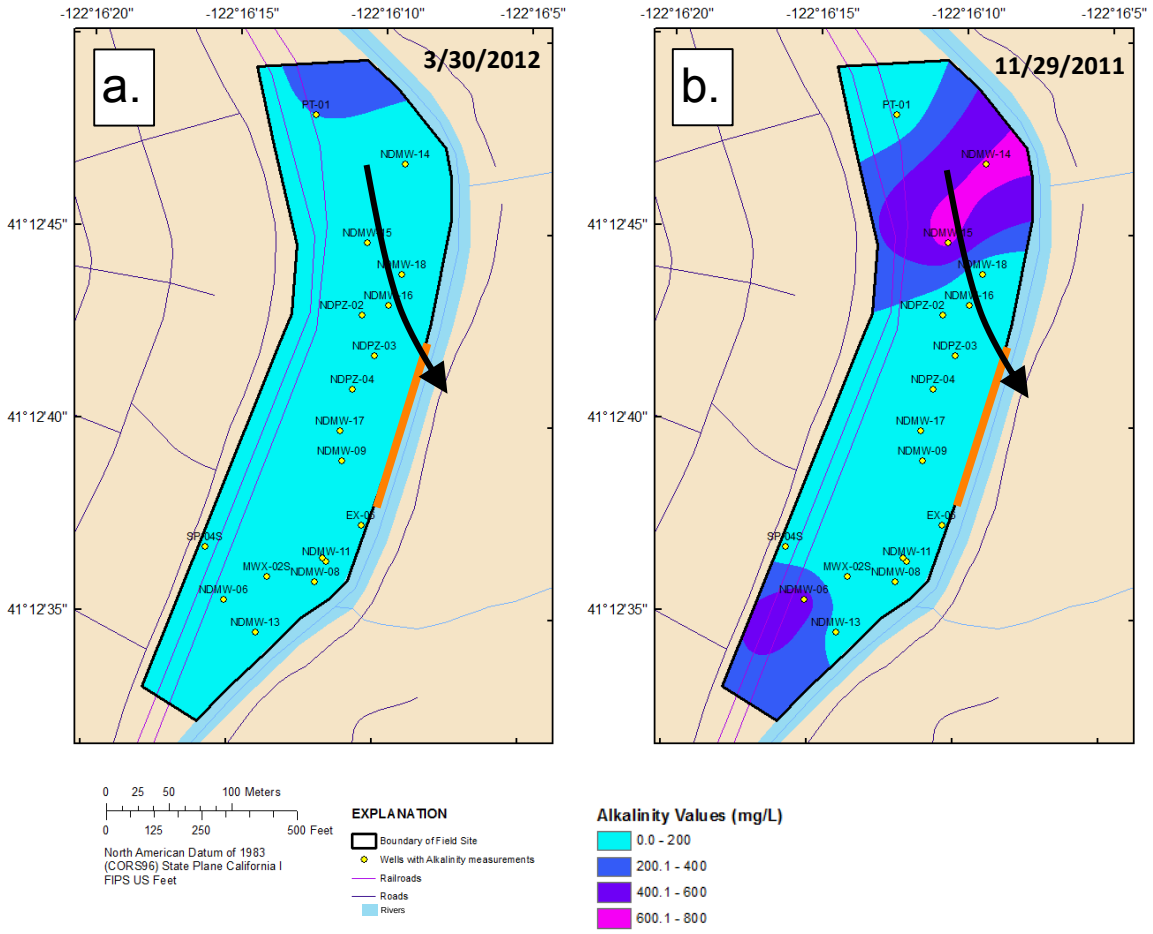

Figure 27. Map showing the alkalinity values in mg/L during high stage flows (left; 27a) vs. baseflow (right; 27b). Black arrow indicates transport pathway, orange line indicates 450' segment with NAPL seeps.

for electron release in the oxidation-reduction reactions. This shows that the highest rates of biodegradation occur in the northern area adjacent to the river during baseflow. However, during high stage flow, products of biodegradation are diluted due to high flow.

CHAPTER VII

DISCUSSION

BASIC HYDROGEOLOGY

The NAPL transport pathway, which is electrically conductive as seen from the site ERI transects, can be explained beginning with the movement and mixing of water through the field site. The site experiences several hydrologic inputs that control the flow of water across the site.

The EMMA analysis coupled with geochemical parameters, such as pH and chloride, indicate that the surface and groundwater entering the site are not significantly different in composition. They are low in dissolved solids, cold (<12°C), and oxic. The mixing analysis determined groundwater at the southern end of the site reflected these regional background waters, while groundwater in the northern end were different. The flow conditions at the northern end of the site are controlled by stream water input, while flow in the southern end is controlled from both stream water and groundwater inputs, which is bounded by an electrically conductive pathway through the center of the site as indicated by ERI data. During stream baseflow, groundwater flow is substantially reduced and the site experiences temperatures above any of the regional groundwater or stream water temperatures and increases in chemical constituents.

The site is periodically disrupted by high stage stream flows, caused by high stream discharge. During high stage flows, groundwater levels are increased by up to 4 m and chemical constituents are relatively homogenized and diluted across the site. The evolution of the chemical constituents

provides a good example of the flow patterns from base flow to high stage flow. The highest concentrated area of the chemical constituents dissipates following a high stage flow and some low concentration areas undergo increases. Therefore, the entire site is flooded and lower temperature water and temporary dilutes the products of biochemical processes. This changing flow regime produces a biogeochemical mixing zone through the site. Similar to the investigation of a gravel system by Miller et al. (2014), the site sees the highest volume flows following high precipitation events that flood the site. During a substantial high stream discharge event the field site is flushed, leaving almost all constituents homogeneous across the site and diluted in the northern end.

The areas of significant biochemical processes can be interpreted from temperature data. The site has elevated temperature measurements in the north central to northeastern area of the field site that rise during base flow conditions and are found to be as much as 20°C when the warmest background in the stream or groundwater is 15°C. The ranges of temperatures at the site are higher than exist in regional background waters. This is interpreted to be caused from heat generation due to in situ biochemical processes and is supported by high concentrations of degradation byproducts, such as CH_4 and S_2, in the northern end of the site (Allen et al., 2007; Yesiller et al., 2005). Yesiller et al. (2005) discussed that an increase in heat content was observed for a specific water content, which was optimal for the system. However if water content was substantially increased over the optimal amount, the heat content decreased. Additionally, Rees (1980) discussed that excessive water in a system could prevent methanogenesis. This suggests the field site has lower biochemical reactions during high flow. Other plausible means of a thermal input were ruled out, such as groundwater thermal inputs or ambient temperature effects.

NAPL TRANSPORT

The chemical constituents found in observation wells can be used as a measure of the extent of biochemical processes during baseflow. The evolution of the chemical constituents at the site allows for conclusions that November 2011 was a time dominated by baseflow with less influence from surface water flow. The northern area adjacent to the stream is interpreted to be the primary area of biochemical reactions. This is observed in the ORP data as well as other elevated byproducts of reduction reactions such as CH_4, S_2, and CO_2. Additionally, elevated temperature, pH, conductivity, and alkalinity further suggest biodegradation of NAPLs. The interpretation of active biochemical processes at the site is also supported by the EMMA analysis. After the appropriate end-members were identified, the analysis demonstrated the northern end of the field site was undergoing chemical reactions altering the parameters and displaying extreme concentrations outside the boundaries of the end-members, while the center and southern end of the site have concentrations more reflective of the chemistry of the end-members.

Reduced stream flow and lower water levels through the site and additional contaminant sourcing to the northern end is a suitable environment for biological activity. There is hypothesized to be additional contaminant sourcing of sulfur from an anthropogenic source, potentially from sulfur diesel fuels, supported by sulfate levels in the northern end of the site that are above stream concentrations. Historical data indicated that the fueling systems were located in the northern area of the site. Major fuel storage and fueling operations at the site were discontinued in 2003. Historically, locomotive diesel fuels could contain over 500 ppm of sulfur (United States Environmental, 2012b).

During baseflow, NAPLs periodically migrate along the preferential pathway caused from the flow regimes discussed above. During high stage flows, the concentrations become nearly homogenous and the elevated concentrations in the northern end become diluted. This is

interpreted as a mechanism that dilutes the products of biochemical reactions undergoing in the northern end of the field site, but refreshes electron acceptors in the site. During high stage flows the site is flooded, also causing dilution and dispersion of NAPLs as well as other chemical constituents. This provides an explanation for the discontinuous appearances of the oil sheens on the Sacramento River and the periodic detection of NAPLs in the existing monitoring wells.

Additional hypotheses that the site is undergoing degradation via microorganisms need additional data to be tested fully. Research would need to be conducted to confirm the microbial community present as well as areas with potential biosurfactant production. The process of biodegradation would produce biosurfactants, which break up and emulsifies the NAPLs, aiding in the transport process and explaining the highly conductive pathway, as discussed by Atekwana et al. (2004). The northeast end of the site is most likely experiencing the highest rates of biodegradation. Therefore, during times of baseflow, NAPLs are hypothesized to transport along the preferential flow path into the river. During high stage flows, the products of biodegradation are diluted and homogenized across the site. It is not clear at this time if the migration is aided by biotransformations of the hydrocarbons (Mohanty and Mukherji, 2008) or by biosurfactant mobilizing hydrocarbon (Banat, 1995) as either mechanism is possible with the existing data.

Characterization Framework

The analysis of this site provides significant insight into a framework for characterization of sheens into surface water as sites with multiple NAPL impacts. The analysis illustrates that chemical and hydrogeologic data, while valuable, could not provide a solid conceptual site model for the site. The additional statistical analysis for mixing and electrical geophysical data provided needed information to understand the causes for the variability in the other datasets. The analysis also indicates that the additional of microbial data regarding populations or the production of biosurfactants would be useful in further strengthening the conceptual model.

The steps to characterize a complex waste site are variable, however there are some basic methods that would contribute to better characterizing the field site in order for the best remediation techniques. Basic physical parameters at this field site were sufficient to understanding the spatial and temporal extent of the increased activity areas at the field site. These included, water levels, temperature, and conductivity, which can be measured with multi-parameter probes. Collection of these parameters should be consistent over time and obtained with other sampled parameters for proper comparison. The elevated temperatures and conductivities above regional groundwater measurements provided support for areas with the highest biochemical reactions within the site. Additionally, water levels demonstrated the flow of groundwater through the site.

Electrical resistivity data was beneficial to isolate the pathway of NAPL transport however understanding if the pathway was produced from geological differences in conductivity or biological was difficult without proper correlation between soil cores or well tests to understand the subsurface permeability variability. Collection of a full suite of cations and anions and contaminant depths and quantities over multiple consistent sample periods would have helped to further characterize the water-rock interactions, biochemical process undergoing, and provide parameters to use in a mixing analysis. The PCA and EMMA analysis performed for the site was limited based on available parameters at the field site and in the regional USGS database. Consistency was the dominant issue with the site parameters. Data were collected at variable dates and well locations. The PCA and EMMA analysis was a cost-effective tool if geochemical parameters are available to further isolate wells or areas that lie outside the background waters of the region. This analysis demonstrated at the field site that the northern end of the site was significantly altered from the sources waters providing evidence of biochemical processes taking place.

The improvements in understanding the site conceptual model provide significant benefits when doing remedial design on these types of sites. Full remediation of these sites with multiple impacts that are still active facilities is complicated. Understanding that temperature and streamflow variability have direct impacts on NAPL migration and the pathway for movement open new remediation strategies that can be employed to limit surface water sheens. Understanding where, when and why the NAPLs are migrating and generating sheens is the first step to cost effective management of the issue.

CHAPTER VIII

CONCLUSION

This research indicates the dominant migration pathway at the site is controlled by complex mixing and flow patterns. The shallow groundwater adjacent to surface water can produce a biochemical mixing zone that create flow pathways tens of meters away from the surface water body. As surface and groundwater sources entered the field site, their magnitude and direction determined the location and type of biochemical reactions that occur. Following high stage flows, the site was flooded with water and dilutes the products of in situ biochemical processes. In contrast, during baseflow the groundwater and stream water flow lines generated a dominant migration pathway. The pathway coincides with the steep chemical gradient line of many geochemical parameters during baseflow. Additionally, this pathway can be seen in ERI transect data as highly electrically conductive. Mixing analysis indicated that the site waters were sometimes significantly different from source waters due to reactions and potential site sources altering the geochemical signatures at the field site.

It was determined that during high stage flows, chemical constituents become homogenized and diluted where elevated. However, during baseflow the chemical constituents become increasingly elevated in the northern end of the site. Therefore, baseflow conditions produced a suitable environment for biochemical reactions to occur in this area.

This disruption in the reactions from high stage flows is mimicked in the output of oil sheens and quantity of NAPLs in extraction wells, which are seen as periodic or discontinuous. This is strongly correlated between the water levels at the site. Higher groundwater levels should limit the surface water sheens. ORP values and other reactants indicate that biodegradation is occurring at the field site. However, future research should be conducted to verify a microbial community as well as the biological processes that would allow for NAPLs to transport to the adjacent stream.

This work suggests several broader conclusions. The basis of understanding a contaminated field site transporting NAPLs is based on the hydrogeology derived from cores, wells, and chemical data. Understanding the subsurface geology in conjunction with the water properties of the area provide a strong foundation to identify the underlying mechanisms of migration. An integrated data framework including statistical analysis, electrical geophysics, and microbial ecology data provide a conceptual site model that would allow for more effective site management.

REFERENCES

Abdel Aal, G., Atekwana, E., Radzikowski, S., Rossbach, S., (2009). Effect of bacterial adsorption on low frequency electrical properties of clean quartz sands and iron-oxide coated sands. Geophysical Research Letters, 36(4).

Abdul, A. S., (1988). Migration of petroleum products through sandy hydrogeologic systems. Groundwater Monitoring & Remediation 8(4): 73-73.

United States Environmental Protection Agency, (2012a, December 12). Glossary of technical terms. Retrieved From the Environmental Protection Agency website: http://www.epa.gov/oust/cat/tumgloss.htm

United States Environmental Protection Agency, (2012b, December 26). Highway and Nonroad Diesel Fuel Standards. Retrieved From the Environmental Protection Agency website: http://www.epa.gov/otaq/fuels/dieselfuels/regulations.htm

Allen, J. P., Atekwana, E. A., Atekwana, E. A., Duris, J. W., Werkeme, D. D., Russbach, S., (2007). The microbial community structure in petroleum-contaminated sediments corresponds to geophysical signatures. Applied and environmental microbiology 73(9): 2860-2870.

Atekwana, E. A., Atekwana, E. A., Rowe, R. S., Werkema Jr., D. D., Legall, F. D., (2004a). The relationship of total dissolved solids measurements to bulk electrical conductivity in an aquifer contaminated with hydrocarbon. Journal of Applied Geophysics 56(4): 281-294.

Atekwana, E. A., Werkema Jr., D. D., Duris, J. W., Rossbach, S., Atekwana, E. A., Sauck, W. A., Cassidy, D. P., Means, J., Legall, F. D., (2004b). In-situ apparent conductivity measurements and microbial population distribution at a hydrocarbon-contaminated site. Geophysics 69(1): 56-63.

Atekwana, E. A., Werkema, D. D., Atekwana, E. A., (2006). Biogeophysics: The effects of microbial processes on geophysical properties of the shallow subsurface. Applied Hydrogeophysics, Springer: 161-193.

Baker, M. B., Grove, T. L., Price, R., (1994). Primitive basalts and andesites from the Mt. Shasta region, N. California: products of varying melt fraction and water content. Contributions to Mineralogy and Petrology 118(2): 111-129.

Banat, I. M., (1995). Biosurfactants production and possible uses in microbial enhanced oil recovery and oil pollution remediation: a review. Bioresource Technology 51(1): 1-12.

Bear, J., (1972). Dynamics of fluids in porous media. Eisevier, New York, 764p.

Bedient, P. B., Rifai, H. S., Newell, C. J., (1999). Ground water contamination: transport and remediation, Prentice-Hall International, Inc.

Bennett, P., Siegel, D. E., Baedecker, M. J., Hult, M. F., (1993). Crude oil in a shallow sand and gravel aquifer—I. Hydrogeology and inorganic geochemistry. Applied Geochemistry 8(6): 529-549.

Birman, I., Alexander, M., (1996). Effect of viscosity of nonaqueous-phase liquids (NAPLs) on biodegradation of NAPL constituents. Environmental toxicology and chemistry 15(10): 1683-1686.

Cassidy, D. P., Werkema Jr, D. D., Sauck, W., Atekwana, E., Rossbach, S., Duris, J., (2001). The effects of LNAPL biodegradation products on electrical conductivity measurements. Journal of Environmental & Engineering Geophysics, 6(1), 47-52.

Christophersen, N., Hooper, R. P., (1992). Multivariate analysis of stream water chemical data: The use of principal components analysis for the end-member mixing problem. Water Resources Research 28(1): 99-107.

Cirmo, C. P., McDonnell, J. J., (1997). Linking the hydrologic and biogeochemical controls of nitrogen transport in near-stream zones of temperate-forested catchments: a review. Journal of Hydrology, 199(1), 88-120.

Cloutier, V., Lefebvre, R., Therrien, R., Savard, M. M., (2008). Multivariate statistical analysis of geochemical data as indicative of the hydrogeochemical evolution of groundwater in a sedimentary rock aquifer system. Journal of Hydrology 353(3): 294-313.

Doctor, D. H., Alexander Jr., E. C., Petric, M., Kogovsek, J., Urbanc, J., Lojen, S., Stichler, W., (2006). Quantification of karst aquifer discharge components during storm events through end-member mixing analysis using natural chemistry and stable isotopes as tracers. Hydrogeology Journal 14(7): 1171-1191.

Driedger, C. L., Kennard, P. M., (1986). Ice Volumes on Cascade Volcanoes: Mount Rainer, Mount Hood, Three Sisters, Mount Shasta. Available from Supt Doc, USGPO, Wash DC 20402. USGS Professional Paper 1365, 1986. 28 p, 27 fig, 6 tab, 28 ref.

ESRI, 2001, ArcGIS spatial analyst—Advanced GIS spatial analysis using raster and vector data, accessed October 29, 2013, at http://www.esri.com/library/whitepapers/pdfs/arcgis_spatial_analyst.pdf.

Fan, W., Yang, Y. S., Du, X. Q., Lu, Y., Yang, M. X., (2011). Finger-printing biodegradation of petroleum contamination in shallow groundwater and soil system using hydro-bio-geochemical markers and modelling support. Water, Air, & Soil Pollution 220(1-4): 253-263.

Fetter, C. W., (1999). Contaminant hydrogeology (Vol. 500). Upper Saddle River, NJ: Prentice hall.

Fitts, C. R., (2002). Groundwater science, Academic Press.

Gentry, J., Laudernilch, D., Diel, J., (2013). Use of Above-Ground Resistivity Mapping to Identify NAPL Migration Pathways. Railroad Environmental Conference, University of Illinois at Urbana-Champaign.

Gentry, J., Halihan, T., McDonald, T., Guidry, L., (2014). Use of Above-Ground Resisitivity Mapping to Identify NAPL Migration Pathways. International Conference on Remediation and Management of Contaminated Sediments, Battelle at New Orleans, Louisiana.

Griesemer, J., (2001). Diving Plumes: The Development an dInvestigation of Dissolved Contaminant Plumes that Migrate Vertically Downward to Depths Below the Water Table. Site Remediation News. Trenton, New Jersey, State of New Jersey, Department of Environmental Protection. 13: 7-12.

Halihan, T., Paxton, S., Graham, I., Fenstemaker, T., Riley, M., (2005). Post-remediation evaluation of a LNAPL site using electrical resistivity imaging. Journal of Environmental Monitoring 7(4): 283-287.

Hirt, W. H., (1999). Quaternary volcanism of Mount Shasta and vicinity, Siskiyou County, California. Weed, College of the Siskiyous.

Hunt, J. R., Sitar, N., Udell, K. S., (1988). Nonaqueous phase liquid transport and cleanup: 1. Analysis of mechanisms. Water Resources Research 24(8): 1247-1258.

Jackson, R. E., Dwarakanath, V., Ewing, J. E., Avis, J., (2006). Migration of viscous non-aqueous phase liquids (NAPLs) in alluvium, Fraser River lowlands, British Columbia. Canadian geotechnical journal 43(7): 694-703.

Laaksoharju, M., Skarman, C., Skarman, E., (1999). Multivariate mixing and mass balance (M3) calculations, a new tool for decoding hydrogeochemical information. Applied Geochemistry 14(7): 861-871.

Leahy, J. G., Colwell, R. R., (1990). Microbial degradation of hydrocarbons in the environment. Microbiological reviews 54(3): 305-315.

Lee, J., Cheon, J., Lee, K., Lee, S., Lee, M., (2001). Factors affecting the distribution of hydrocarbon contaminants and hydrogeochemical parameters in a shallow sand aquifer. Journal of contaminant Hydrology 50(1): 139-158.

Legall, F. D., (2002). Geochemical and isotopic characteristics associated with high conductivities in a shallow hydrocarbon-contaminated aquifer.

Malard, F., Tockner, K., Ward, J. V., (1999). Shifting dominance of subcatchment water sources and flow paths in a glacial floodplain, Val Roseg, Switzerland. Arctic, Antarctic, and Alpine Research, 135-150.

McBirney, A. R., White, C.M., (1982). The Cascade province. New York, John Wiley and Sons.

Miller, R. B., Heeran, D. M., Fox, G. A., Halihan, T., Storm, D. E., (2014). The hydraulic conductivity structure of gravel-dominated vadose zones within alluvial floodplains. Journal of Hydrology 513: 229-240.

Mohanty, G., Mukherji, S., (2008). Biodegradation rate of diesel range n-alkanes by bacterial cultures Exiguobacterium aurantiacum and Burkholderia cepacia. International Biodeterioration & Biodegradation, 61(3), 240-250.

Mullaney, J. R., Lorenz, D. L., Arntson, A. D., (2009). Chloride in groundwater and surface water in areas underlain by the glacial aquifer system, northern United States. Reston, VA: US Geological Survey.

Newell, C. J., Acree, S. D., Ross, R. R., Huling, S. G., (1995). Ground Water Issue: Light Nonaqueous Phase Liquids. U. S. E. P. Agency. Washington, DC.

Newman, B. D., Campbell, A. R., Wilcox, B. P., (1998). Lateral subsurface flow pathways in a semiarid ponderosa pine hillslope. Water Resources Research, 34(12), 3485-3496.

Nichols, E., Roth, T., (2006). Downward Solute Plume Migration, Assessment, Significance, and Implications for Characterization and Monitoring of "Diving Plumes". API Soil and Groundwater Technical Task Force, Bulleting 24.

Poole, G. C., Stanford, J. A., Running, S. W., Frissell, C. A., (2006). Multiscale geomorphic drivers of groundwater flow paths: subsurface hydrologic dynamics and hyporheic habitat diversity. Journal of the North American Benthological Society, 25(2), 288-303.

Rifai, H. S., Bedient, P. B., Wilson, J. T., Miller, K. M., Armstrong, J. M., (1988). Biodegradation modeling at aviation fuel spill site. Journal of Environmental Engineering 114(5): 1007-1029.

Ron, E. Z., Rosenberg, E., (2001). Natural roles of biosurfactants. Environmental microbiology 3(4): 229-236.

Sefa, V., (2015). Mechanisms for detecting NAPL in groundwater with resistivity. Master thesis: Oklahoma State University. Retrieved from ProQuest Dissertations and Theses.

Segers, R., (1998). Methane production and methane consumption: a review of processes underlying wetland methane fluxes. Biogeochemistry, 41(1), 23-51.

Spence, M. J., Bottrell, S. H., Thornton, S. F., Richnow, H. H., Spence, K. H., (2005). Hydrochemical and isotopic effects associated with petroleum fuel biodegradation pathways in a chalk aquifer. Journal of contaminant hydrology, 79(1), 67-88.

Streck, M. J., Keeman, W. P., Chesley, J., (2007). High-magnesian andesite from Mount Shasta: A product of magma mixing and contamination, not a primitive mantle melt. Geology 35(4): 351-354.

Sudsaeng, S., Yimsiri, S., Flores, G., Katsumi, T., Inui, T., Likitlersuang, S., (2011). Diesel migration in sand under groundwater movements. Kasetsart University, Thailand.

U.S. Geological Survey, 2014, National Water Information System data available on the World Wide Web (USGS Water Data for the Nation), accessed [September 12, 2014], at URL [http://waterdata.usgs.gov/nwis/].

Valder, J. F., Long, A. J., Davis, A. D., Kenner, S. J., (2012). Multivariate statistical approach to estimate mixing proportions for unknown end members. Journal of Hydrology 460: 65-76.

Walter, V., Syldatk, C., Hausmann, R., (2010). Screening concepts for the isolation of biosurfactant producing microorganisms. Biosurfactants, Springer: 1-13.

Weaver, J. W., Wilson, J. T., (2000). Diving plumes and vertical migration at petroleum hydrocarbon release sites. LUST Line Bulletin 36.

Wagner, D. L., Saucedo, G. J., (1987). California Geological Survey, Regional Geologic Map, No. 4A, 1:250,000 scale.

Williams, H., (1932). Mount Shasta, a Cascade volcano. The Journal of Geology: 417-429.

Wondzell, S. M., Swanson, F. J., (1996). Seasonal and storm dynamics of the hyporheic zone of a 4th-order mountain stream. I: Hydrologic processes. Journal of the North American Benthological Society, 3-19.

Wroblicky, G. J., Campana, M. E., Valett, H. M., Dahm, C. N., (1998). Seasonal variation in surface-subsurface water exchange and lateral hyporheic area of two stream-aquifer systems. Water Resources Research, 34(3), 317-328.

Yeşiller, N., Hanson, J. L., Liu, W., (2005). Heat generation in municipal solid waste landfills. Journal of Geotechnical and Geoenvironmental Engineering.

YSI, Inc., (2013). Biochemical reactions and corresponding ORP values. https://www.ysi.com/ysi-blog/water-blogged-blog/2013/08/orp-management-in-wastewater-as-an-indicator-of-process-efficiency.

APPENDICES

APPENDIX A
DISCHARGE GRAPHS

This data set contains available chemical constituents from monitoring well NDMW-14 at the northern end of the field site with stream discharge data from the Sacramento River at the Lakehead site approximately 25 miles south of the field site (40.93972°N, -122.41611°W).

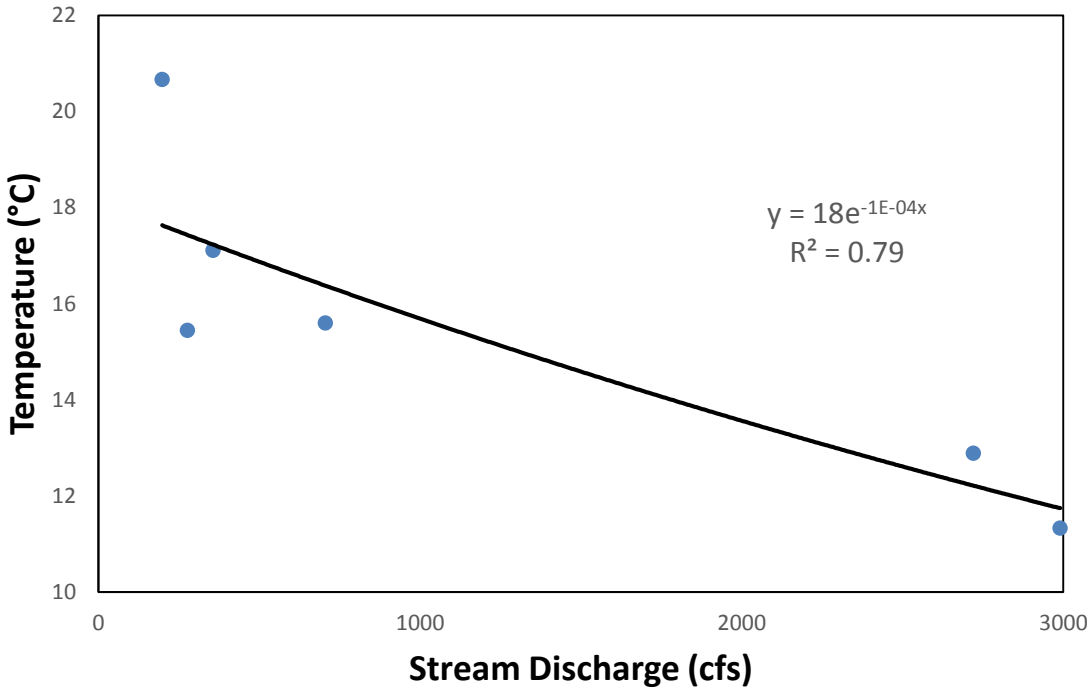

Figure A-1. Graph showing the daily stream discharge of the Sacramento River approximately 25 miles south of the field site at the Lakehead location with temperature measurements from a well in the north central area of the field site, NDPZ-03.

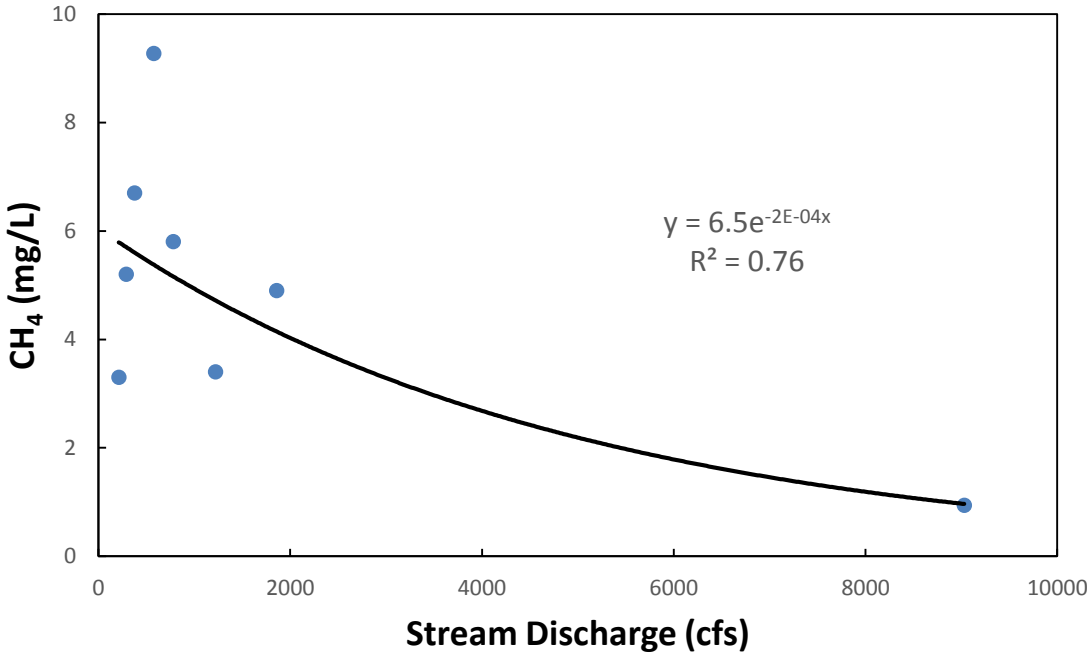

Figure A-2. Graph showing the daily stream discharge of the Sacramento River approximately 25 miles south of the field site at the Lakehead location with CH_4 measurements from a well in the north central area of the field site, NDMW-14.

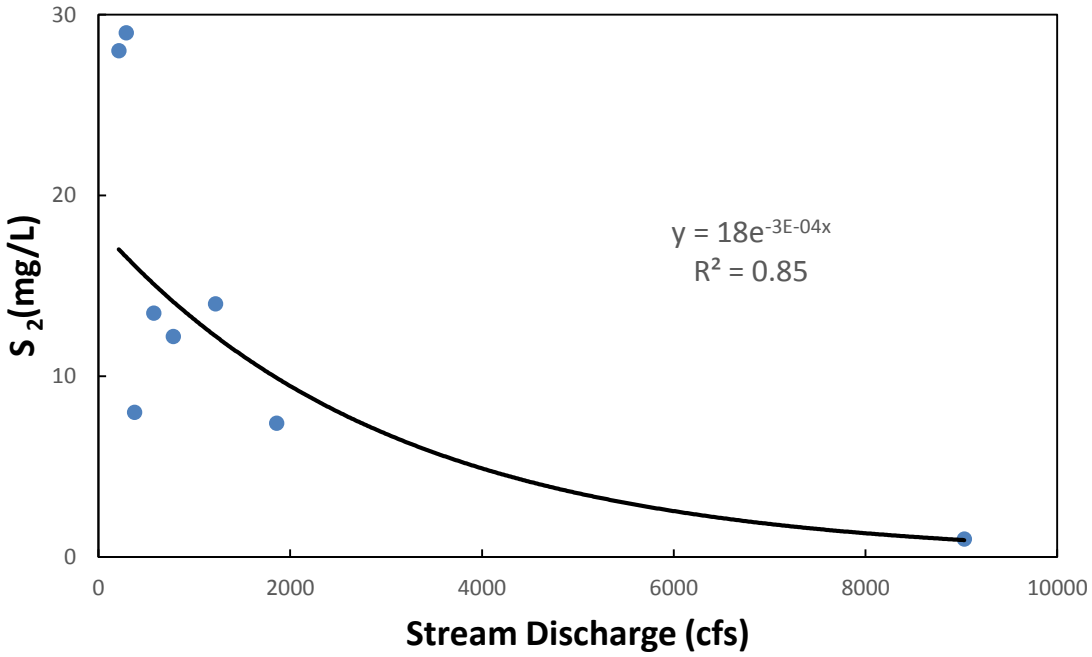

Figure A-3. Graph showing the daily stream discharge of the Sacramento River approximately 25 miles south of the field site at the Lakehead location with S_2 measurements from a well in the north central area of the field site, NDMW-14.

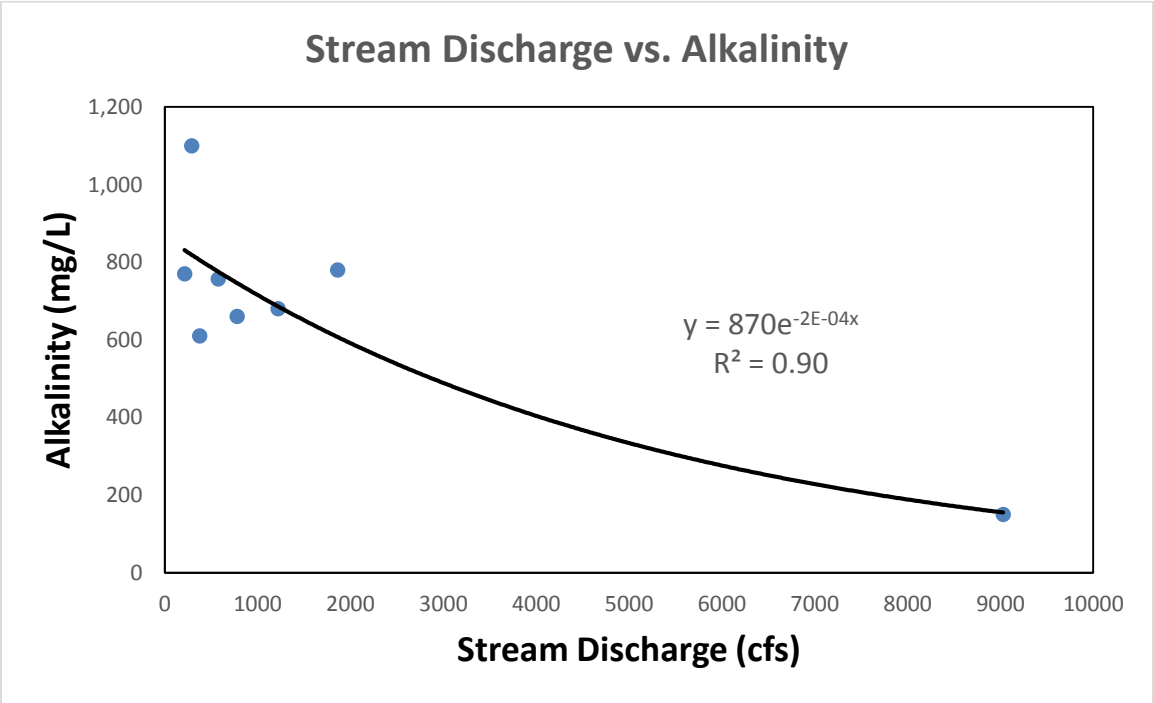

Figure A-4. Graph showing the daily stream discharge of the Sacramento River approximately 25 miles south of the field site at the Lakehead location with alkalinity measurements from a well in the north central area of the field site, NDMW-14.

VITA

Lauren N. Guidry

Candidate for the Degree of

Master of Science

Thesis: CONTROLS ON NAPL MIGRATION PATHWAYS IN A MIXED-WASTE RAIL YARD, DUNSMUIR, CALIFORNIA

Major Field: Geology

Biographical:

Education: Received a Bachelor of Science degree in geology from Oklahoma State University in Stillwater, Oklahoma in 2012. Completed the requirements for the Master of Science in geology at Oklahoma State University, Stillwater, Oklahoma, in July 2015.

Experience: Employed as a hydrogeology intern for the Oklahoma Water Resources Board in Oklahoma City, Oklahoma, from September 2012 to March 2014. Employed as a petroleum geology intern for Noble Energy, Inc. from May 2014 to August 2014.

Professional Memberships: Geological Society of America, American Association of Petroleum Geologists, Association for Women Geoscientists, Tulsa Geological Society, and Oklahoma City Geological Society.